KfK 4007
Dezember 1985

Break Up of Light Ions in the Nuclear and Coulomb Field of Nuclei

D. K. Srivastava
Institut für Kernphysik

Kernforschungszentrum Karlsruhe

KERNFORSCHUNGSZENTRUM KARLSRUHE

Institut für Kernphysik

KfK 4007

BREAK UP OF LIGHT IONS IN THE NUCLEAR AND COULOMB FIELD OF NUCLEI*

D.K. Srivastava[+]

[+] On leave from Variable Energy Cyclotron Centre, Calcutta, India

* Lectures presented at the XVII[th] International Summer School on Nuclear Physics, Mikolajki, Poland, Sept. 1985

Kernforschungszentrum Karlsruhe GmbH, Karlsruhe

Kernforschungszentrum Karlsruhe GmbH
Postfach 3640, 7500 Karlsruhe 1

ISSN 0303-4003

ABSTRACT

The break up of light ion projectiles in the nuclear and Coulomb field of nuclei is considered. Current theoretical concepts for describing break up processes and their theoretical features are discussed. An alternative method, based on a prior-interaction DWBA, is introduced for the calculation of the direct elastic break up cross sections. This method reveals the role of the internal momentum distribution of the break up fragments and includes corresponding "finite range" effects.
The Coulomb break up of ^{6}Li is studied on the basis of a quasi-sequential break up approach (following Rybicki and Austern) and results are obtained for very low relative energies of the emerging α-particles and deuteron fragments. The astrophysical interest in these cross sections is noted. A view on further extensions of the break up theory is given.

DER AUFBRUCH LEICHTER IONEN IM NUKLEAREN UND COULOMBFELD VON KERNEN

Zusammenfassung

Der Aufbruch leichter Projektilionen im nuklearen und Coulombfeld von Atomkernen wird betrachtet. Die gängigen theoretischen Konzepte zur Beschreibung der Aufbruchprozesse und ihre Grundsätze werden beschrieben und diskutiert. Eine alternative Methode, die auf der prior-Wechselwirkung der DWBA beruht, wird eingeführt, um den direkten elastischen Aufbruch zu beschreiben. Diese Methode verdeutlicht die Rolle der inneren Impulsverteilung der Aufbruchfragmente und schließt "finite range"-Effekte ein.
Der Aufbruch von ^{6}Li im Coulombfeld wird auf der Basis eines quasisequentiellen Aufbruchmodells (nach Rybicki und Austern) studiert, und Resultate bei sehr geringen Relativenergien der auslaufenden α-Teilchen und Deuteronen werden gewonnen. Das astrophysikalische Interesse an diesen Wirkungsquerschnitten wird notiert. Der weitere Ausbau der Theorie wird angedeutet.

CONTENTS

"Nun zerbrecht mir das Gebäude,
Seine Absicht hat's erfüllt..."

Friedrich Schiller,
Das Lied von der Glocke

1. INTRODUCTION

Break up of loosely bound composite projectiles in the field of a target nucleus[1,2] has been found to contribute substantially to the total reaction cross-section of nucleus-nucleus collisions. This phenomenon is often signalled by a broad and pronounced peak (see fig. 1) in the inclusive spectrum of the emitted particles, with an energy corresponding approximately to the beam velocity. A large fraction of the break up reaction is ascribed to nonelastic processes, where only one projectile fragment is emitted, while the other interacts inelastically with the target nucleus, in particular by forming a fused system in preequilibrium and equilibrium stages. Elastic break up processes (see fig. 2) with the target nucleus left in the ground state has been experimentally studied by measuring the coincidence spectrum of the two projectile fragments following the break up reaction. In addition to the interest in a detailed understanding of the reaction mechanism and of the origin of various components observed in the continuum spectra, we have the interesting question about the extent to which we may learn anything from the momentum distributions and differential cross-sections about the cluster motion of the two fragments. This is a long standing question, and arises from the historically first formulation[3] of the projectile break up theory in terms of a plane wave approximation.

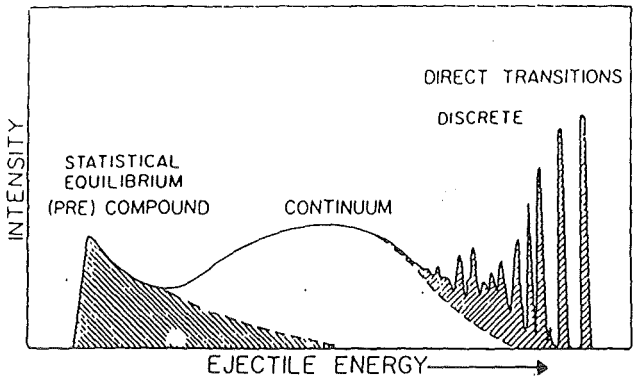

A schematic particle energy spectrum at a forward angle

I do not know what I may appear to the world, but to myself I seem to have been only a boy playing on the sea-shore, and diverting myself in now and then finding a smoother pebble or a prettier shall than ordinary, whilst the great ocean of truth lay all undiscovered before me.

Sir Isaac Newton
(1642-1727)

- Memoirs of Newton, Vol.II, ch.27

FIGURE 1 A schematic particle energy spectrum at a forward angle and the importance of break up processes.

A proper understanding of the break up processes is not only important for its own sake. In fact, it is a prerequisite for a quantitative understanding of such interesting phenomena as giant resonances and deep lying single particle states[4], the spectra for which are partly submerged in the break up continuum. The relative abundances of the break up of a particular projectile in various modes may also provide information about the relative strengths of various

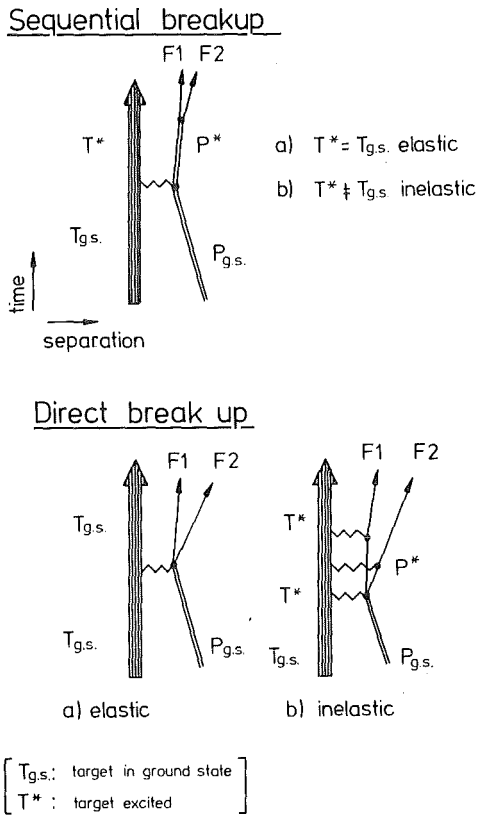

FIGURE 2 Illustration of sequential and direct break up processes.

possible clusterpartitions of the projectile as say for ^{6}Li which may decompose into (α+d), (α+p+n), (^{3}He+t), (^{5}Li+n), (^{5}He+p) etc.

Most importantly, break up studies may provide a very strong impetus to the understanding of nuclear reactions of astrophysical interest[5]. Traditional nuclear physics experiments have often great difficulties to provide quantitative and accurate information about such reactions due to the

very low relative energies involved and the associated uncertainties and experimental difficulties in detection, especially due to low cross-sections (see fig. 3). Break up reactions can prove to be very handy in two ways. This is best illustrated by means of examples. Consider the astrophysically important reaction

$$p + {}^{20}Ne \rightarrow {}^{21}Na \qquad (1.1)$$

We need to know the cross-section for this reaction for very low E_p, which has its associated problems as mentioned above. However, if we study the break up reaction

$$d + {}^{20}Ne \rightarrow p + {}^{20}Ne + n \qquad (1.2)$$

the three-body exit channel provides us with a flexibility to choose any $E(p-{}^{20}Ne)$ by selecting kinematical conditions. However, we can use high energy deuterons which, acting as the "Trojan Horse", would carry protons above the Coulomb barrier[6]. The attempt to relate the relevant cross section have only been started.

The other and more promising method is to use the break up reactions (especially the Coulomb break up where the situation is much more clean) as the inverse process[5] of capture reactions of astrophysical importance. Consider for example the reaction

$$^{7}Be + {}^{208}Pb \rightarrow \alpha + {}^{3}He + {}^{208}Pb \qquad (1.3)$$

which can be used to get information about the reaction,

$$\alpha + {}^{3}He \rightarrow {}^{7}Be + \gamma \qquad (1.4)$$

for low relative energies. The kinematics for the reaction (1.3) for a particular $(\alpha-{}^{3}He)$ angle pair is shown in fig. 4. It is quite clear that one can choose very low relative values for $E_{\alpha-{}^{3}He}$ even though E_α and $E_{{}^{3}He}$ remain quite large

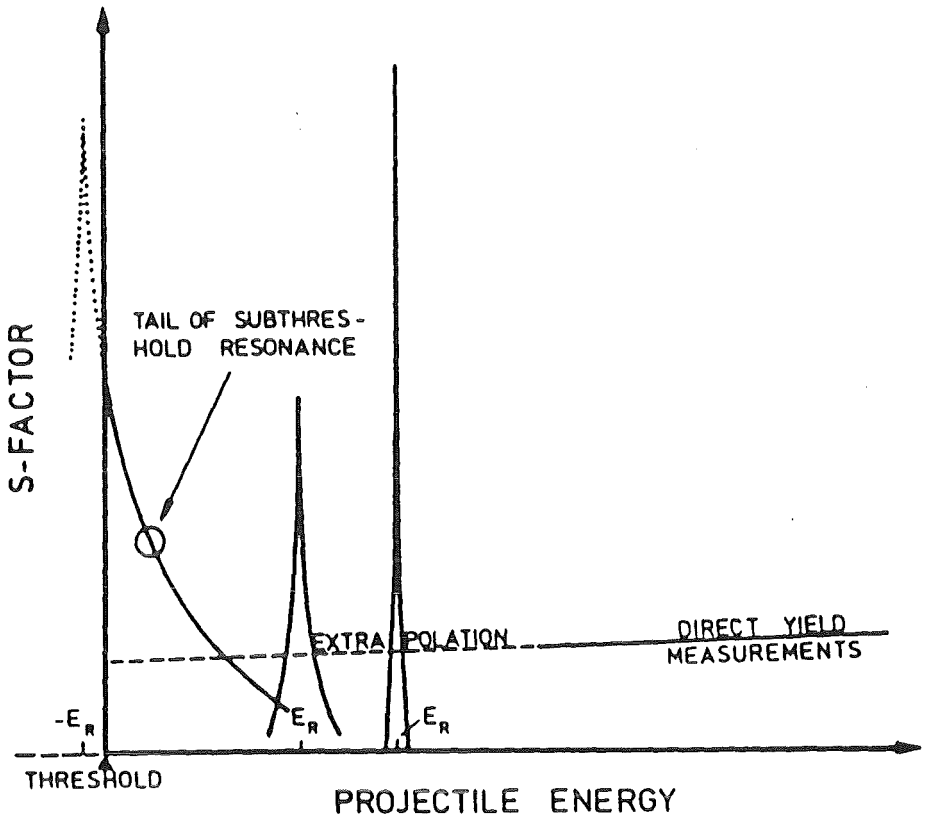

FIGURE 3 Illustration of the problem of low energy direct capture reaction. The present estimates rely heavily on the extrapolation.

and thus very easy to measure accurately. Then for a pure Coulomb-break up, the break up cross section, which can possibly be treated as excitation to a continuum level with energy $E_{\alpha-^3He}$ can be written

$$\sigma_{bu}(E_{\alpha-^3He}) = N(E_{\alpha-^3He}, E_{^7Be})\ \sigma^{(\gamma)}(E_{\alpha-^3He}) \qquad (1.5)$$

where N(E',E) is the number of virtual quanta per unit energy E' in the electromagnetic field of the charged projectile (moving with energy E), which are available for excitation

and $\sigma^{(\gamma)}(E')$ is the photo-excitation cross section ^{7}Be going to $(\alpha-^3\mathrm{He})^*$. This $\sigma^{(\gamma)}$ is related to the direct capture cross section for the process (1.4) by

$$\sigma(\alpha+^3\mathrm{He}\rightarrow{}^7\mathrm{Be}+\gamma) = \frac{(2j_{^7\mathrm{Be}}+1)\ 2\ k_\gamma^2 \cdot\sigma^{(\gamma)}(E_{\alpha-^3\mathrm{He}})}{(2j_\alpha+1)\ (2j_{^3\mathrm{He}}+1)\ k^2_{\alpha-^3\mathrm{He}}} \qquad (1.6)$$

where symbols have their usual meaning. A reliable estimate of σ_{bu} is essential for this procedure to be of help. In Table I, we give a list of reactions which may be studied in this manner. We would like to add that the virtual photon density N increases with the energy, and therefore the method would be much more effective at higher incident energies.

TABLE I Break up reactions of astrophysical interest[5].

Coulomb break up as inverse reaction		
Reaction	Q	Remark
^{7}Be $+^3$He	- 1.586 MeV	Solar Neutrino-Problem
^{13}N p+^{12}C	- 1.94 MeV	
^{17}F p+^{16}O	- 0.60 MeV	CNO-Cycle
^{14}O p+^{13}N	- 4.62 MeV	
^{21}Na p+^{20}Ne	- 2.43 MeV	
^{19}Ne $+^{15}$O	- 3.53 MeV	Break up for the RP-process
^{18}F $+^{14}$N	- 4.42 MeV	Helium-Burning
^{20}Ne $+^{16}$O	- 4.73 MeV	

In section 2, we shall have a look at some of the coincidence and inclusive data from literature to get a feeling of the break up process. In sect. 3, we give a formal derivation of post- and prior-forms of the break up T-matrix

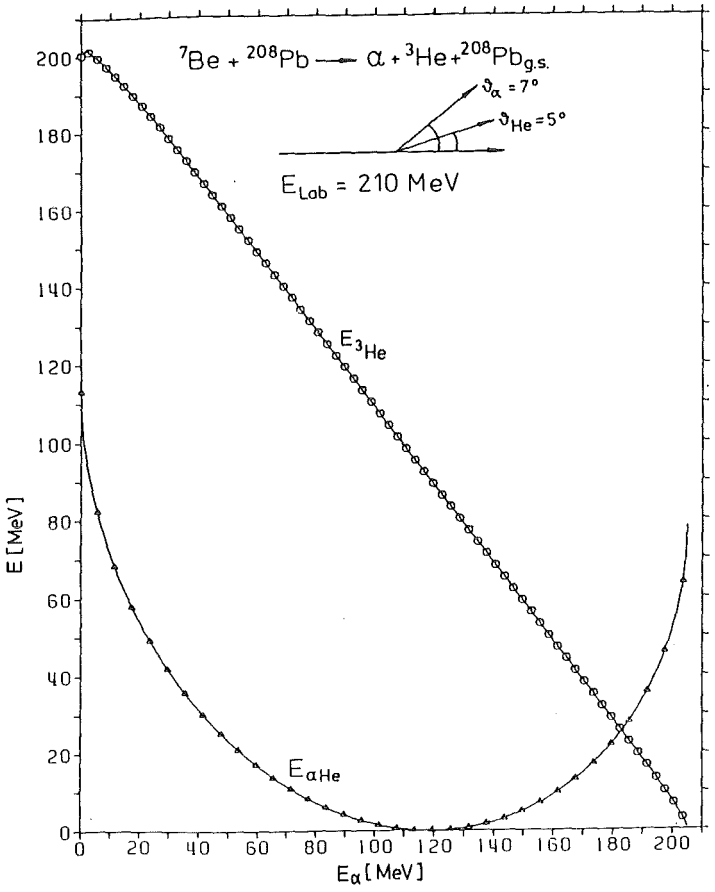

FIGURE 4 The kinematics for the elastic break up of ^{7}Be (210 MeV) in the field of ^{208}Pb. Relative energies can be chosen at will by choosing the angles of measurement.

and the difficulties associated with them. In sect. 4, we shall give our procedure to deal with the prior-form of the DWBA T-matrix for the break up process and discuss the results and their significance.

The Coulomb break up is discussed in sect. 5 and a particularly beautiful situation which arises for break-up, $^{6}Li \rightarrow \alpha + d$ is discussed in sect. 6.

2. GLIMPSES OF EXPERIMENTAL DATA

Let us just have a look at some of the experimental data available in literature, to get a feeling of the reaction mechanism. Due to the three body situation of the exit channel, we can have either kinematically incomplete measurements represented by inclusive spectra, or kinematically complete measurements resulting in coincidence or exclusive spectra. The coincidence spectra are generally taken for the situation, when the target is left in its ground state, i.e. for the elastic break up processes.

In fig. 5, one of the first coincidence measurements of break up of deuterons at an incident energy of 12 MeV from a target of gold nuclei is shown. The shifts of the peak positions from the beam-velocity can be understood from the fact that in the entrance channel deuteron is de-accelerated by the Coulomb field while in the exit channel proton is accelerated by the same field.

In fig. 6, similar measurements for 56 MeV deuterons from ^{51}V are shown. Now the peak positions are not shifted too much from the beam-velocity positions as the energies involved are much higher.

In fig. 7, we have an example of coincidence measurements of break up of ^{3}He from the ^{28}Si nuclei, at 52 MeV. The peaks do not occur at the beam velocity due to low energies and the acceleration effects mentioned above.

Fig. 8 shows inclusive measurements for the $(^{3}He,d)$ process on ^{90}Zr for 90 MeV ^{3}He projectile. Unlike the above mentioned case, here the peak lies very close to the beam velocity, as the energy is high enough to make Coulomb-considerations irrelevant. Even the tightly bound α-particle breaks up at high incident energies as can be seen from the inclusive spectrum of the 172 MeV α-particles incident upon nickel

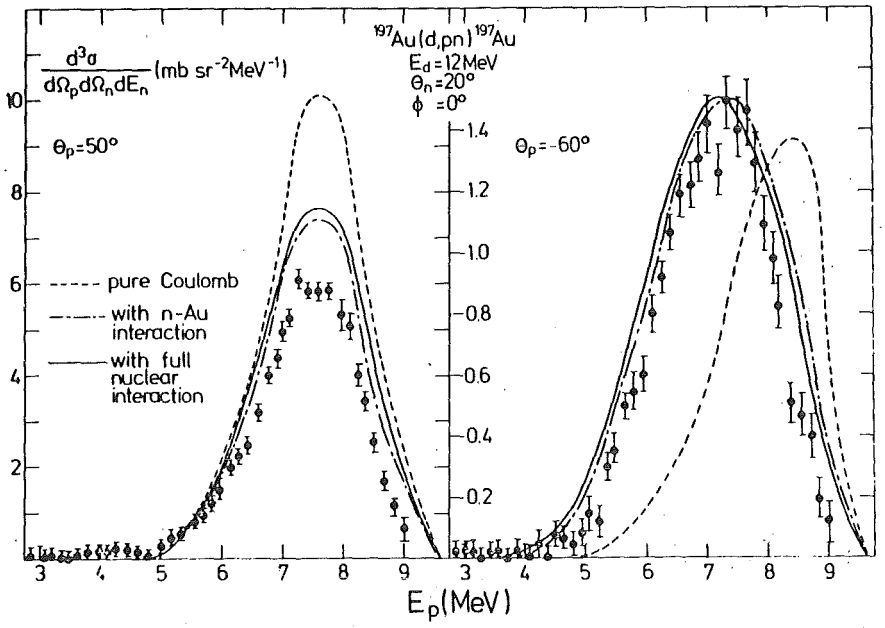

FIGURE 5 Deuteron break up coincidence cross-section on ^{197}Au at E_α = 12 MeV (Jarcyk et al.). Most of the theoretical predictions up to fig. 13 are using the theories of Baur's school, to be discussed later.

target. The break up bump is fairly well formed at forward angles, and possibly other processes have started contributing at higher angles (Fig. 9). The inclusive break up spectrum for low energy ^{9}Be is shown in Fig. 10. The shift in the peak-position due to Coulomb barrier is quite noticable here. All the basic features of break up can be seen.

The study of break up of ^{6}Li has been taken up in a systematic exploration at Karlsruhe. The inclusive spectra for the break up of ^{6}Li into α+d at 156 MeV from ^{40}Ca and

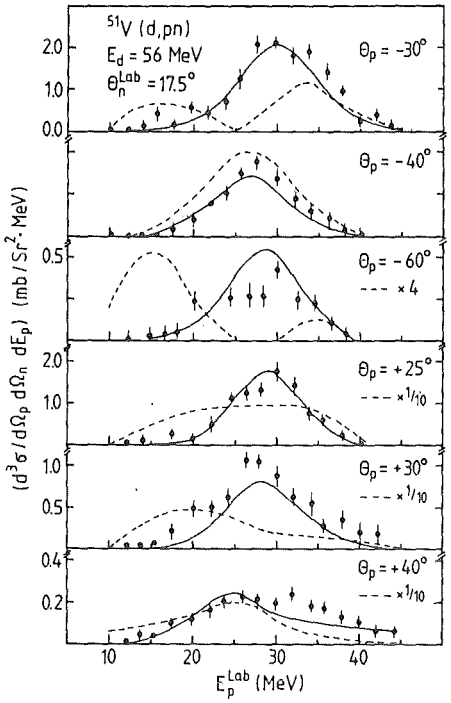

FIGURE 6
Deuteron break up coincidence cross-section on ^{51}V at E_d = 56 MeV from Matsuoka et al.[8] The solid lines show the theoretical predictions of the Baur's school[1] where as the dashed lines show the predictions of Austern's school.[16]

^{208}Pb at various angles are shown, respectively in fig. 11 and 12. We see very clearly, the evolution of the break up bump as the angle of observation is reduced. In other words, as the angle has increased the contribution from nondirect processes has become important. However, when the break up bump is present it is very close to E_α = 104 MeV emphasizing the beam-velocity supposition.

The inclusive break up data for the ^{208}Pb target[13] are again plotted in fig. 13 for a better perspective. The cross section is seen to drop very rapidly from 12° to 22°, but is peaked at E_α = 104 MeV, as seen before, This emphasizes the direct nature of break up processes.

Some measurements can be seen from contributions to this conference[15].

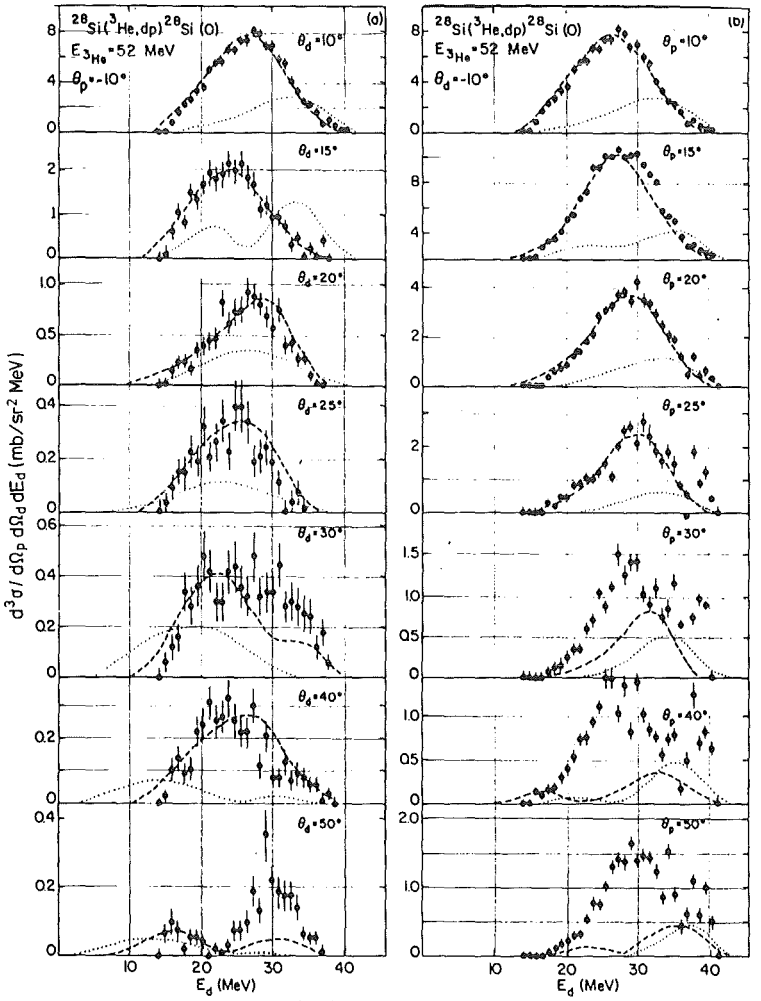

Projected energy spectra for the ^{28}Si(^{3}He, pd) elastic breakup for θ_p fixed at $\theta_p = -10°$ (a) and θ_d fixed at $\theta_d = -10°$. (b).

FIGURE 7 Triple differential cross sections for $^{28}Si(^{3}He,dp)^{28}Si$ reaction at $E_{^3He}$=52 MeV with theoretical predictions of the quasifree break up model (Aarts et al.[9]).

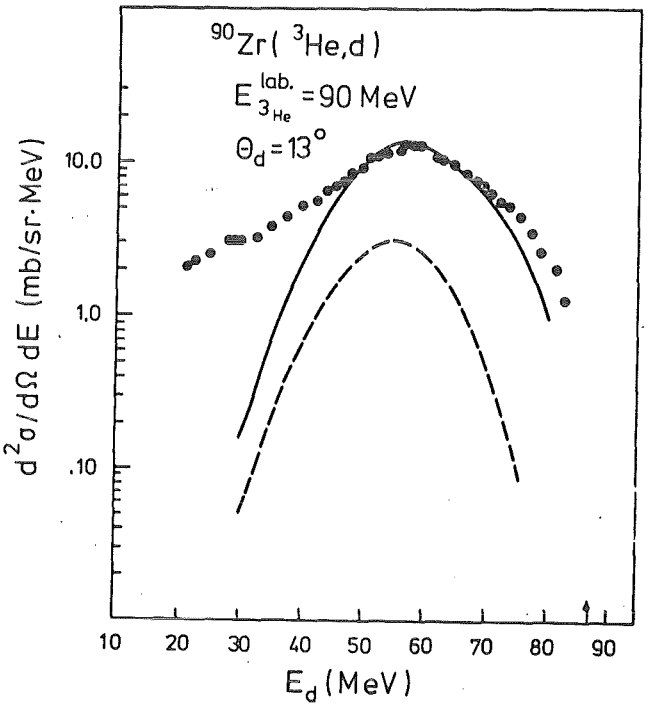

FIGURE 8 Inclusive measurements of (^{3}He,d) cross-section on ^{90}Zr target at $E_{^3He}$ = 90 MeV (Matsuoka et al.[10]).

3. THE FORMAL DWBA THEORY FOR BREAK UP.

Let us consider, the elastic break up of the projectile

$$a = b + x \tag{3.1}$$

in the field of the nucleus A,

$$a + A \rightarrow b + x + A \tag{3.2}$$

The total Hamiltonian for this situation is written as

$$H = T_b + T_x + U_{bA} + U_{xA} + V_{bx} + H_A + H_b + H_x \tag{3.3}$$

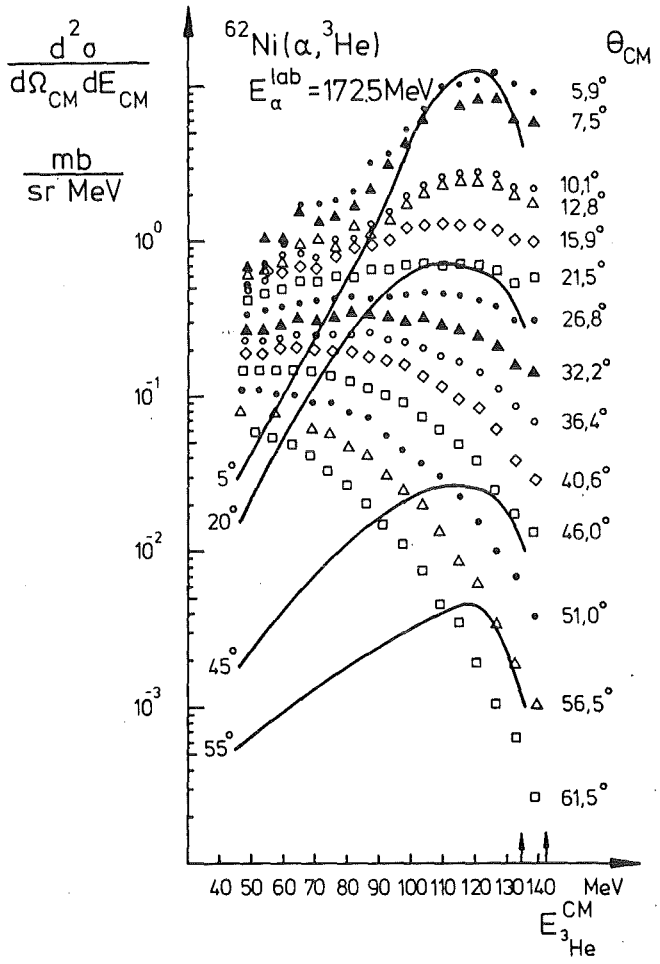

FIGURE 9 Inclusive measurements for the break up of 172 MeV α-particles (Budzanowski et al.[11]).

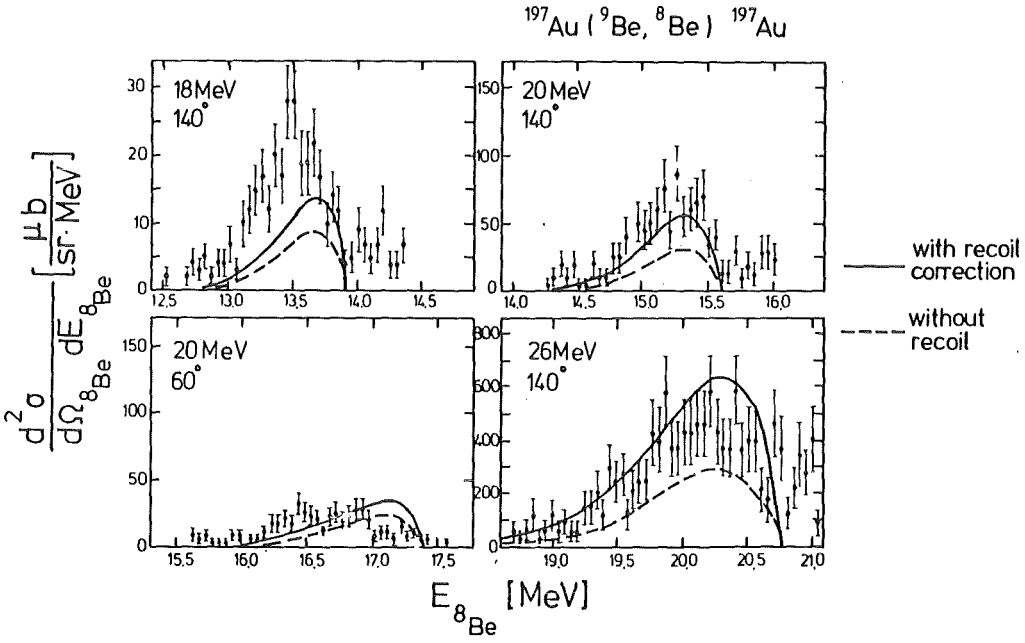

FIGURE 10 Sub-Coulomb break up of ^{9}Be from ^{197}Au. (Unternährer et. al.[12]).

where T_b and T_x denote the kinetic energy operators for b and x, H_A, H_b, H_x are the internal Hamiltonians of A, b and x which are treated as being inert later on. V_{bx} is the interaction binding the projectile and U_{BA} and U_{xA} are approximated to be the optical model potentials for the b + A and x + A systems respectively.

We immediately see that the Hamiltonian H contains three interaction terms and it is very difficult to have a solution of such a 3-body situation. Two distinct "schools" have emerged according to the way they approximate this 3-body situation to a more tractable two-body situation. For convenience we shall call them Baur's[1] ans Austern's

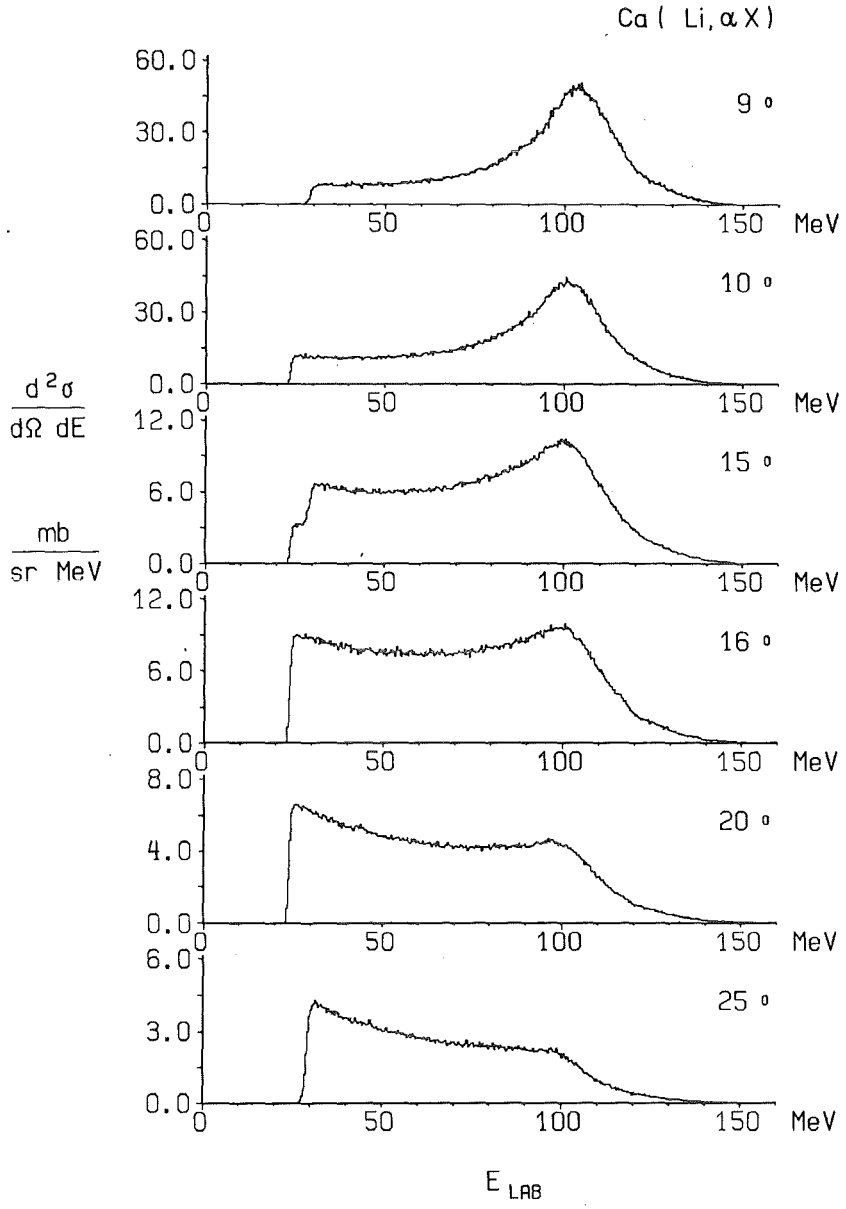

FIGURE 11 Inclusive α-particle spectra of the break up of ^{6}Li from ^{40}Ca at 156 MeV, observed at various emission angles.

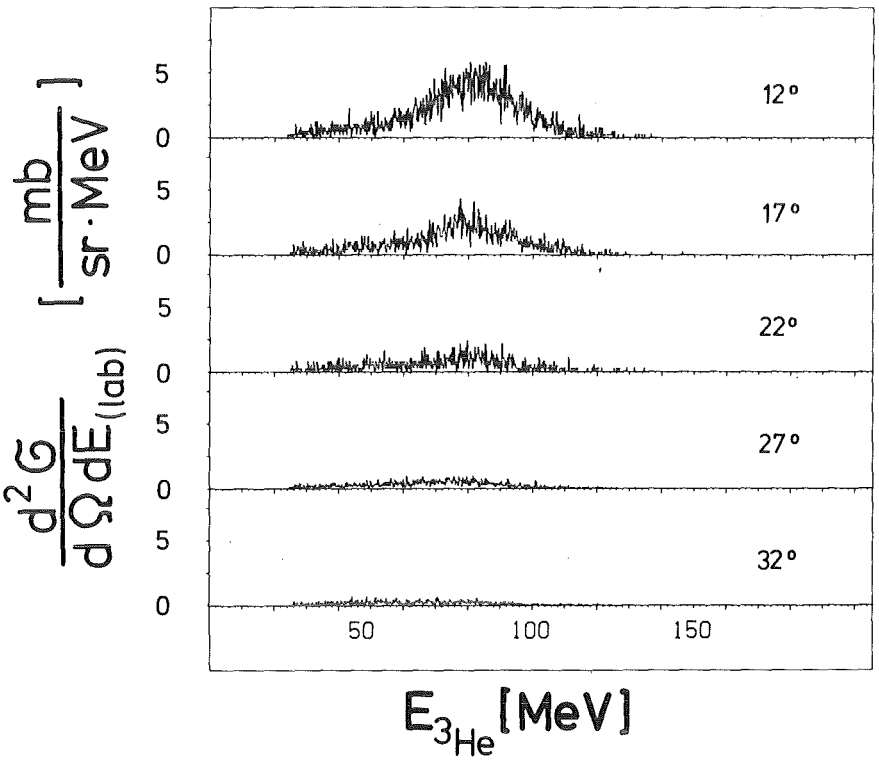

FIGURE 12 Same as Fig. 11 for a ^{208}Pb target

schools[16], respectively. Thus the calculations performed by Baur and coworkers[1] rest upon the assumption that V_{bx} is weak and can be neglected while writing the solution of the full Hamiltonian for the exit channel. Austern's school[16,8,17,18] on the other hand approximates $U_{bA} + U_{xA}$ by a potential U_{aA} describing the centre of mass motion of the fragments b and x in the exit channels (see fig. 14) The basic limitations of the two schools becomes evident immediately when we note that the interaction V_{bx} between b and x can not be ignored when their relative energy is small (e.g.

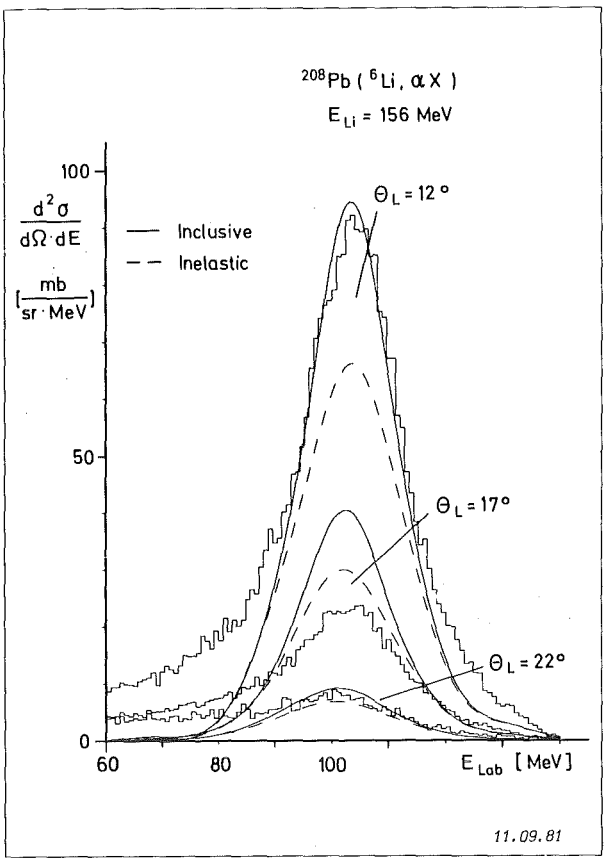

FIGURE 13 Angular distribution of the inclusive measurements of break up of ^{6}Li at 156 MeV from ^{208}Pb.

when the Coulomb repulsion will play a very important role), and it is hard to visualize an optical model potential which would describe the centre of mass motion of two free particles. With this in mind, we derive the transition matrix for the two schools in the following. Some authors prefer

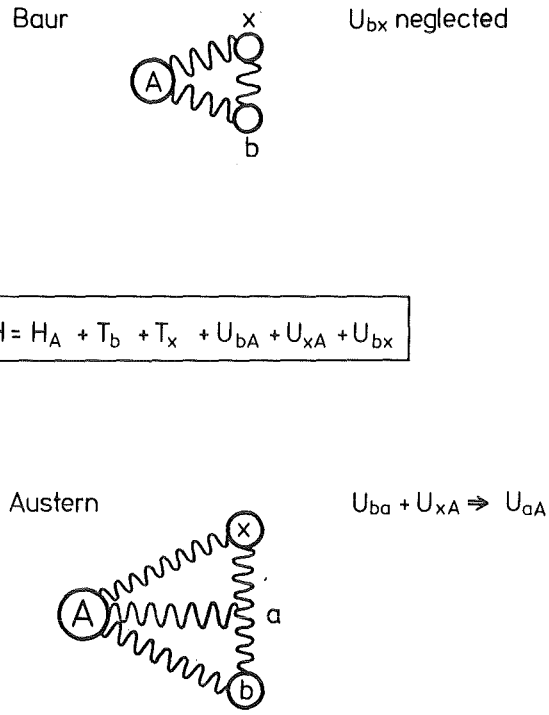

FIGURE 14 The approximations invoked by Baur and Austern to reduce the three body problem of break up to a two body situation.

to call the calculations performed using Baur's theories as direct break up while the calculations performed using Austern's approach are called sequential break up. These are also known as post- and prior-forms of the DWBA theories, respectively. The origin of these names would become more evident, lateron.

3.1 T-matrix for Baur's school.

In this case, the Hamiltonian for the initial state is written as

$$H_i = H_A + T_b + T_x + H_b + H_x + V_{bx}$$
$$= H_A + H_a + T_a \qquad (3.4)$$

and the corresponding Hamiltonian for the final state is written as

$$H_f = H_A + T_b + T_x + H_b + H_x \qquad (3.5)$$

and we note that V_{bx} is not included in H_f, as discussed above. Now the initial and final state interactions are given as

$$V_i = H - H_i$$
$$= U_{bA} + U_{xA} \qquad (3.6)$$

and

$$V_f = H - H_f$$
$$= U_{bA} + U_{xA} + V_{bx} \qquad (3.7)$$

The exact transition matrix in the prior-interaction form is given by

$$T_{fi}^{(-)} = \langle \Psi_f^{(-)} \mid V_i \mid \phi_i \rangle \qquad (3.8)$$

where $\Psi_f^{(-)}$ is the full solution of the Hamiltonian H with only ingoing boundary conditions and ϕ_i is solution of the free Hamiltonian in the ingoing channel,

$$\phi_i = \psi_A \cdot \psi_a \cdot \exp\,(i\,\vec{k}_a \cdot \vec{r}_{aA}) \qquad (3.9)$$

where ψ_A and ψ_a are ground state wave functions of the target and the projectile respectively, $\vec{k}_a$ is the free wave number in the incident channel and $\vec{r}_{aA}$ is the projectile-target separation.

The equivalent post-form of the exact transition matrix is given by

$$T_{fi}^{(+)} = < \phi_f \mid V_f \mid \Psi_i^{(+)} > \qquad (3.10)$$

where similarily $\Psi_i^{(+)}$ is the full solution of the Hamiltonian H with outgoing wave boundary conditions, ϕ_f as the solution of the free Hamiltonian H_f, in the exit channel and is given by

$$\phi_f = \psi_A \cdot \psi_b \cdot \psi_x \cdot \exp(i \vec{k}_b \cdot \vec{r}_{bA} + i \vec{k}_x \cdot \vec{r}_{xA}). \qquad (3.11)$$

In the above $\vec{k}_b$ and $\vec{k}_x$ are the free-wave numbers of b and x and $\vec{r}_{bA}$ and $\vec{r}_{xA}$ are the distances of b and x from the target A, which is considered to be infinitely heavy.

Now the Gellmann-Goldberger theorem can be used to give,

$$T_{fi}^{(-)} = < \Psi_f^{(-)} \mid U_{bA} + U_{xA} - U_{aA} \mid \psi_a \cdot \psi_A \cdot \chi_a^{(+)} > \qquad (3.12)$$

where $\chi_a^{(+)}$ is the distorted wave for the (auxiliary) optical model potential U_{aA} for the projectile a with an outgoing wave boundary condition.

Similarily, we also get,

$$T_{fi}^{(+)} = < \psi_A \psi_B \psi_x \chi_b^{(-)} \cdot \chi_x^{(-)} \mid V_{bx} \mid \Psi_i^{(+)} > \qquad (3.13)$$

The corresponding prior-DWBA matrix is obtained by approximating

$$\Psi_f^{(-)} \approx \psi_A \cdot \psi_b \cdot \psi_x \cdot \chi_b^{(-)} \cdot \chi_x^{(-)} \qquad (3.14)$$

in (3.12) and we get after performing the integration over the internal co-ordinates

$$T_{fi}^{(-)} \text{ (DWBA)} = <\chi_b^{(-)} \cdot \chi_x^{(-)} \mid U_{bA} + U_{xA} - U_{aA} \mid \phi_a \cdot \chi_a^{(+)}> \qquad (3.15)$$

where ϕ_a is the relative motion wave-function of the fragments b and x in the ground state of the projectile a.

The corresponding post-form of the DWBA matrix is obtained by approximating,

$$\psi_i^{(+)} \approx \psi_a \cdot \psi_A \cdot \chi_a^{(+)} \tag{3.16}$$

which leads to, after integration over internal co-ordinates,

$$T_{fi}^{(+)}\ (\text{DWBA}) = \langle \chi_b^{(-)} \cdot \chi_x^{(-)} \mid V_{bx} \mid \chi_a^{(+)} \cdot \phi_a \rangle \tag{3.17}$$

It has been demonstrated by Huby and Mines[19] on quite general grounds that the forms (3.15) and (3.17) are equivalent to each other.

Baur et al.[1] have evaluated the form (3.17), the so-called post-form, with the additional assumption of a zero-range approximation, which gives,

$$V_{bx}(r_{bx}) \cdot \phi_a(\vec{r}_{bx}) = D_o \delta(\vec{r}_{bx}) \tag{3.18}$$

and implies that

$$\phi_a(\vec{r}_{bx}) = \sqrt{2\alpha} \cdot \frac{e^{-\alpha r_{bx}}}{r_{bx}} \cdot Y_{oo}(\Omega_{bx}) \tag{3.19}$$

with

$$\alpha = \sqrt{\frac{2\mu_{bx}\,\varepsilon}{\hbar^2}} \tag{3.20}$$

where ε is the binding energy. Thus, a zero-range approximation implies that the relative motion of b and x is confined a L=0 orbit with the radial wave-function given by a Yukawa-function, whose parameters are completely determined by the binding energy. This of course in turn limits the momentum-distribution of b and x to a Lorentzian shape $\propto 1/(k^2+\alpha^2)$ which is a rather serious limitation of the theory, since break up processes are observed equally frequently for heavier projectiles whose relative motion wave-function does not conform to the above restriction. On the other side, an

exact finite range calculation does not seen to be feasible using the expression (3.17) as the contribution comes from all over the space requiring a contour integration even with a zero range approximation.

The corresponding prior-form has not been used till recently due to the complexity of co-ordinate transformation. Later, we shall see that it can be evaluated fairly easily and provides interesting insights in addition to retaining full details of the projectile wave-function which insures an implicit exact treatment of the finite range effects.

3.2 T-matrix for Austern's school

In this case, the Hamiltonian for the initial state is written as before (3.4) as

$$\begin{aligned} H_i &= H_A + T_b + T_x + H_b + H_x + V_{bx} \\ &= H_A + H_a + T_a \end{aligned}$$

however, the corresponding Hamiltonian for the final state is written as

$$H_f = H_A + T_b + T_x + H_b + H_x + V_{bx} \tag{3.20}$$

and we note that V_{bx} is retained in H_f, implying a final-state interaction between b and x in the exit channel. Thus the initial state interaction is given by

$$\begin{aligned} V_i &= H - H_i \\ &= U_{bA} + U_{xA} \end{aligned} \tag{3.21}$$

and the final state interaction is

$$\begin{aligned} V_f &= H - H_f \\ &= U_{bA} + U_{xA} \quad = \quad V_i \end{aligned} \tag{3.22}$$

We see that the solution of the free Hamiltonian in the in-

going channel is still given by (3.9). However, the appropriate solution for the free Hamiltonian in the final state is,

$$\phi_f = \psi_A \cdot \psi_a' \cdot \exp(i \vec{k}_a' \cdot \vec{r}_{aA}) \tag{3.23}$$

where ψ_a' describes a continuum wave-function for the system 'b+x' and $\vec{k}_a'$ is the wave-vector for its centre of mass motion.

Now the exact T-matrix is given by

$$T_{fi}^{(-)} = \langle \Psi_f^{(-)} | U_{bA}+U_{xA} | \psi_A \cdot \psi_a \cdot \exp(i \vec{k}_a \cdot \vec{r}_{aA}) \rangle \tag{3.24}$$

and

$$T_{fi}^{(+)} = \langle \psi_A \cdot \psi_a' \exp(i \vec{k}_a' \cdot \vec{r}_{aA}) | U_{bA}+U_{xA} | \Psi_i^{(+)} \rangle \tag{3.25}$$

As before, we use Gell-Mann-Goldberger relation to reduce the plane-waves in (3.24) and (3.25) above and then make DWBA approximations

$$\Psi_i^{(+)} \approx \chi_a^{(+)} \psi_A \cdot \psi_a \tag{3.26}$$

and

$$\Psi_f^{(-)} \approx \chi_{a'}^{(-)} \cdot \psi_A \cdot \psi_{a'} \tag{3.27}$$

for the above T-matrices. The integration over the internal coordinates yields,

$$T_{fi}^{(-)}(\text{DWBA}) = \langle \chi_{a'}^{(-)} \cdot \phi_k^{(-)} | U_{bA}+U_{xA}-U_{aA} | \chi_a^{(+)} \cdot \phi_a \rangle \tag{3.28}$$

and

$$\begin{aligned} T_{fi}^{(+)}(\text{DWBA}) &= \langle \chi_{a'}^{(-)} \cdot \phi_k^{(-)} | U_{bA}+U_{xA}-U_{aA} | \chi_a^{(+)} \cdot \phi_a \rangle \\ &\equiv T_{fi}^{(-)} \cdot (\text{DWBA}) \end{aligned} \tag{3.29}$$

where $\chi_{a'}^{(-)}$ is the scattering wave function describing the centre of mass motion of the fragments b and x in the exit channel and $\phi_k^{(-)}$ describes their relative motion in the continuum.

3.3 Comparison of the T-matrices of the two schools

Before we compare the details of the T-matrices of the two schools, we would like to make the following clarifying comment.

It should be emphasized that the T-matrices (3.8), (3.10), (3.24) and (3.25) are formally identical inspite of different partitions H_i and H_f used in writing them *provided* we use *exact* and full 3-body wave function for Ψ, which is a solution of the full Hamiltonian H. Thus, the two approaches mentioned above emerge from the distorted waves Born approximations where a particular channel is emphasized.

A straight forward understanding of the two schools of break up is obtained by noting that Baur's calculations correspond to stripping of the fragment x into the continuum of the target, though not with a sharp L-value. On the other hand the evaluations of Austern's school correspond to the excitations of the projectile a to its own continuum, followed by decay (see fig. 15).

Yet another interesting aspect is that as $\phi_k^{(-)}$ is a proper scattering wave-function in the potential V_{bx}, we see that Austern's formulation explicitly includes the final state interaction between the broken-up fragments, to all orders.

This is in contrast to the expression (3.17) (or the equivalent expression (3.15)) of Baur's school where the final state interaction V_{bx} is included only up to first order. The zero-range approximation (3.18) further compromises the final-state interaction. The expression (3.15) which does not require such a zero-range approximation retains the final state interaction to first order (due to its equivalence to (3.17). However, this aspect is not quite transparent from this expression.

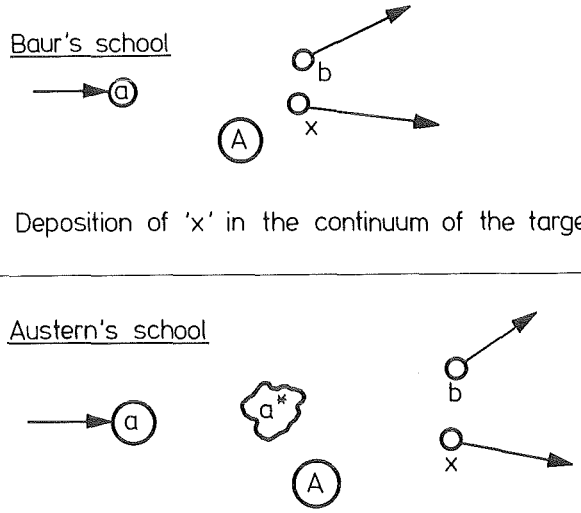

FIGURE 15 The two different physical pictures implied by the prescriptions of Baur and Austern.

3.4 Unusual optical model potential needed for Austern's approach.

In fig. 6, the predictions of Baur's school and Austern's school for the break up of 56 MeV deuterons from ^{51}V are shown. It is seen that the "prior-form" theory is not able to explain the data, where as the post-form theory provides a quantitative explanation of the coincidence spectrum. Similar situation is known for a number of cases where the two theories have been used. Austern et al. have made a detailed

effort to understand this aspect[20]. We would like to sketch the following argument from Austern[21] which effectively explains this discouraging aspect of the prior-form, and traces its failure to the requirement of unusual optical model potential describing the motion of two fre fragments.

Let us take the exact T-matrix for Austern's school (3.25), reduce the plane-wave in the exit channel and suppress internal co-ordinates to write,

$$T_{fi}^{(+)} = \langle \phi_k^{(-)} \; \chi_a^{(-)} | U_{bA}+U_{xA}-U_{aA} | \psi_i^{(+)} \rangle \tag{3.30}$$

where $\chi_a^{(-)}$ is scattering state in the optical potential U_{aA}. The full wave function $\psi_i^{(+)}$ can be expanded as,

$$\psi_i^{(+)} = \chi_a^{(+)} \cdot \phi_a + \int d\vec{k} \; \chi_a^{(+)} \cdot \phi_k^{(+)} \tag{3.31}$$

The DWBA expression (3.29) is obtained by writing

$$\psi_i^{(+)} \approx \chi_a^{(+)} \; \phi_a \tag{3.32}$$

Demanding the full T-matrix (3.30) to be identical to this DWBA expression we get

$$U_{aA} \cdot \chi_a^{(+)} = \int d\vec{k} \; \langle \phi_k^{(-)} | U_{bA}+U_{xA} | \chi_a^{(+)} \cdot \phi_{k'}^{(+)} \rangle \tag{3.33}$$

We see that U_{aA} has to be obtained from a continuum-continuum coupling which indeed is appropriate for a 3-body situation, and is quite different from usual optical model potential. Coupled channels calculations performed along the lines of Sakuragi et al.[36] or an adiabatic treatment similar to that of Austern et al.[20] more or less account for this deficiency.

4. THE PRIOR-INTERACTION DWBA FOR DIRECT BREAK UP OF LIGHT IONS

We noticed earlier that the direct break up model of Baur's school has been used in its post-form for these studies, in conjunction with a zero range approximation. From fig. 13 , one can easily see that the zero-range approximation is not able to reproduce the angular distribution correctly. It is definitively not applicable when the internal cluster motion is not confined to a relative s-state. A full finite-range evaluation of the matrix element

$$T_{\vec{q}_a \to \vec{q}_b \vec{q}_x} = \int \chi_b^{(-)*}(\vec{r}_{bA})\ \chi_x^{(-)*}(\vec{r}_{xA})\ U_{bx}(r_{bx})\ \phi_a(\vec{r}_{bx}) \cdot \chi_a^{(+)}(\vec{r}_{aA})\ d\vec{r}_{aA}\ d\vec{r}_{bx} \qquad (4.1)$$

for the elastic break up reaction

$$a + A \to b + x + A$$

is hardly feasible as the $d\vec{r}_{aA}$-integral converges very slowly, and a straight-forward evaluation may involve integrations up to a few hundred fms. The approximations developed for heavy-ion transfer reactions[22] to handle the above 6-dimensional integral are not suitable for the present situation, since the contributions to the transition matrix element above cannot be limited to a narrow region near the classical turning point (as it may happen for normal transfer reactions, and enabling simplifications like a local momentum approximation).

We have analysed[37] the possibility to overcome the mentioned drawbacks by a reformulation of the DWBA break up theory on the basis of the prior-form prescripton of the T matrix,

$$T_{\vec{q}_a \to \vec{q}_b \vec{q}_x} = \int \chi_b^{(-)*}(\vec{r}_{bA}) \chi_x^{(-)*}(\vec{r}_{xA}) \; [U_{bA}(r_{bA}) + U_{xA}(r_{xA}) - U_{aA}(r_{aA})] \; \phi_a(\vec{r}_{bx}) \; \chi_a(\vec{r}_{aA}) \; d\vec{r}_{aA} \; d\vec{r}_{bx} \qquad (4.2)$$

which is formally equivalent to the post-form expression (4.1). In the past, the prior-form has been discussed in context of the Coulomb-break up of the deuteron[23], where the final state may be described by a Coulomb wave function and a plane wave for the break up neutron. The quasifree break up model applied by Groningen group[9] uses Coulomb corrected plane waves for the projectile and spectator scattering states (and neglects the Coulomb break up).

In this work we consider the full DWBA matrix element (eq. 4.2) without using the various approximations above. The consistent success of the identically equivalent post-form theory of Baur et al. (where the zero-range approximation is admissible) holds out the hope of the unique utility for cases where finite range effects become important and carry interesting information.

The evaluation of the prior-form DWBA matrix element (Eq. 4.2) involves the evaluations of well behaved integrals with contributions from a limited region of space, thus enabling the application of one of the many factorizing techniques for reducing the six dimensional integrals to a finite sum of products of two three dimensional integrals. For this purpose several methods have been proposed and applied. After a careful scrutiny of the methods available we adopted[24] the plane-wave expansion technique devised by Robson and co-workers[25]. It is interesting to note that with this method orbital dispersion effects are seen very clearly. Thus, we express the distorted-waves as a sum of plane-waves (partial

wave by partial wave), over the region $[0,R_{max}]$ and write

$$\chi^{(+)}_{\underline{\ }}(\vec{k},\vec{r}) = 4\pi\Sigma_{LM} i^L \frac{u^{(+)}_{L\underline{\ }}(kr)}{kr} Y^*_{LM}(\hat{k})\, Y_{LM}(\hat{r}) \qquad (4.3)$$

for the case neglecting spin-orbit potential. Now we expand

$$\frac{u^{(+)}_{L\underline{\ }}(kr)}{kr} = \sum_{n=1}^{N(L)} a^{(+)}_{nL\underline{\ }}\, j_L(k_n r) \qquad r \leq R_{max} \qquad (4.4)$$

where

$$a^{(+)}_{nL\underline{\ }} = \sum_{n'=1}^{N(L)} N^L_{nn'}\, b^{(+)}_{n'L\underline{\ }} \qquad (4.5)$$

$$b^{(+)}_{nL\underline{\ }} = k^{-1} \int_0^{R_{max}} r\,dr\, u^{(+)}_{L\underline{\ }}(kr)\, j_L(k_n r) \qquad (4.6)$$

$$N^L_{nn'} = \left|\underline{\underline{\{O(L)\}}}\right|^{-1}_{nn'} \qquad (4.7)$$

and

$$O^{(L)}_{nn'} = \int_0^{R_{max}} r^2 dr\, j_L(k_n r)\, j_L(k_{n'} r) \qquad (4.8)$$

and finally we get,

$$\chi^{(+)}_{\underline{\ }}(\vec{k},\vec{r}) = \sum_{LM} Y^*_{LM}(\hat{k}) \cdot \{ \sum_{nn'} N^L_{nn'}\, b^{(+)}_{n'L\underline{\ }} \int d\hat{k}_n\, e^{i\vec{k}_n\cdot\vec{r}} \cdot Y_{LM}(\hat{k}_n)\} \qquad (4.9)$$

We notice that with such a plane-wave representation, the co-ordinate transformation becomes quite easy.

Taking advantage of the plane-wave representation, we evaluate the T-matrix by integrating the three terms originating from the three optical-model potentials U_{bA}, U_{xA} and U_{aA} over $d\vec{r}_{bx}\cdot d\vec{r}_{bA}$, $d\vec{r}_{bx}\cdot d\vec{r}_{xA}$ and $d\vec{r}_{bx}\cdot d\vec{r}_{aA}$, respectively. The

T-matrix reduces to,

$$T = T_b + T_x - T_a \tag{4.10}$$

or

$$T = \sum_{\substack{L_a L_b L_x \\ M_a M_b M_x}} B \cdot Y^*_{L_a M_a}(\hat{q}_a)\, Y_{L_b M_b}(\hat{q}_b)\, Y_{L_x M_x}(\hat{q}_x) \tag{4.11}$$

with

$$B = \sum_{\substack{n_a\, n'_a \\ n_b\, n'_b \\ n_x\, n'_x}} N^{(+)}_{n_a n'_a,\, b_{n'_a} L_a} \cdot N^{(-)*}_{n_b n'_b,\, b_{n'_b} L_b} \cdot N^{(-)*}_{n_x n'_x,\, b_{n'_x} L_x}$$

$$\int d\hat{k}_{n_a}\; d\hat{k}_{n_b}\; d\hat{k}_{n_x}$$

$$Y_{L_a M_a}(\hat{k}_{n_a})\; Y^*_{L_b M_b}(k_{n_b})\; Y^*_{L_x M_x}(\hat{k}_{n_x})$$

$$\left| \bar{\tilde{V}}_{bA}(P)\tilde{\phi}(\vec{Q}_b) + \tilde{V}_{xA}(P)\tilde{\phi}(\vec{Q}_x) - \tilde{V}_{aA}(P)\cdot\tilde{\phi}(\vec{Q}_a) \right| \tag{4.12}$$

where

$$\tilde{V}_{iA}(P) = \int U_{iA}(r) \cdot \exp(i\,\vec{P}\cdot\vec{r})\, d\vec{r} \tag{4.13}$$

$$\tilde{\phi}(\vec{Q}_i) = \int \phi_a(\vec{r}) \cdot \exp(i\,\vec{Q}_i\cdot\vec{r})\, d\vec{r} \tag{4.14}$$

and

$$\vec{P} = \vec{k}_{n_a} - \vec{k}_{n_b} - \vec{k}_{n_x} \tag{4.15}$$

$$\begin{aligned} \vec{Q}_b &= -\frac{m_x}{m_a}\cdot\vec{k}_{n_a} + \vec{k}_{n_x}, \qquad \vec{Q}_x = \frac{m_b}{m_a}\cdot\vec{k}_{n_a} - \vec{k}_{n_b} \\ \vec{Q}_a &= -\frac{m_x}{m_a}\cdot\vec{k}_{n_b} + \frac{m_b}{m_a}\cdot\vec{k}_{n_x} \end{aligned} \tag{4.16}$$

These equations demonstrate in most clear terms the shape of results to be obtained in this theory. We immediately notice that the maximum of T is decided by the terms for which the expansion coefficients are largest and the momenta $\vec{P}$ and $\vec{Q}_i$ are small.

These considerations lead us to the central result of the break up phenomena, that, unless the orbital dispersion is not too large for the effective partial waves, which are the surface ones (or, in other words the "on-shell" choice $\vec{k}_{n_a} \approx \vec{k}_a$ etc. is a good approximation), a peak in the cross section should be obtained when $E_b \approx \frac{m_b}{m_a} \cdot E_a$ and $E_x \approx \frac{m_x}{m_a} \cdot E_a$. Thus the "beam-velocity-bump" is transparent in our treatment.

Assuming a relative s-state for the projectile wavefunction and taking the z-axis along the incident beam direction we get

$$T = \sum_{\substack{L_a L_b L_x \\ M_x}} N \; T_{L_a L_b L_x} \begin{pmatrix} L_x & L_a & L_b \\ M_x & o & -M_x \end{pmatrix} \cdot \sqrt{\frac{2L_a+1}{4\pi}} \; Y_{L_b -M_b}(\Theta_b, \phi_b) \; Y_{L_x M_x}(\theta_x, \phi_x) \tag{4.17}$$

where

$$T_{L_a L_b L_x} = (4\pi)^3 \sum_{\ell_1 \ell_2 \ell_3 L} i^{\ell_1+\ell_2+\ell_3} (-)^{\ell_2+\ell_3+L} [L]^2 \cdot \left\{ G_b \cdot V^b_{\ell_1 \ell_2 \ell_3} \cdot \phi^b_L + G_x \cdot V^x_{\ell_1 \ell_2 \ell_3} \cdot \phi^x_L - G_a \, V^a_{\ell_1 \ell_2 \ell_3} \right\} \tag{4.18}$$

and

$$G_b = [\hat{\ell}_1 \hat{\ell}_3]^2 \cdot \begin{pmatrix} L_a & \ell_1 & L \\ 0 & 0 & 0 \end{pmatrix} \begin{pmatrix} L_b & \ell_1 & \ell_3 \\ 0 & 0 & 0 \end{pmatrix} \begin{pmatrix} L_x & 3 & L \\ 0 & 0 & 0 \end{pmatrix} \tag{4.19}$$

$$(-)^{L_b} \cdot \delta_{\ell_2 L_b} \cdot W(L_a\ \ell_1\ L_x\ \ell_3\ L \ell_b)$$

$$G_x = [\ell_1 \ell_2]^2 \cdot \begin{pmatrix} L_a & \ell_1 & L \\ 0 & 0 & 0 \end{pmatrix} \begin{pmatrix} L_b & \ell_2 & L \\ 0 & 0 & 0 \end{pmatrix} \begin{pmatrix} L_x & \ell_1 & \ell_2 \\ 0 & 1 & 0 \end{pmatrix} \tag{4.20}$$

$$(-)^{L_x} \delta_{3 L_x} \cdot w(L_b\ \ell_2\ L_a\ \ell_1\ L\ L_x)$$

and

$$G_a = [\hat{\ell}_2 \hat{\ell}_3]^2 \cdot \begin{pmatrix} L_a & \ell_2 & \ell_3 \\ 0 & 0 & 0 \end{pmatrix} \begin{pmatrix} L_b & \ell_2 & L \\ 0 & 0 & 0 \end{pmatrix} \begin{pmatrix} L_x & \ell_3 & L \\ 0 & 0 & 0 \end{pmatrix} \tag{4.21}$$

$$(-)^{L_a} \delta_{\ell_1 L_a} \cdot W(L_x\ \ell_3\ L_b\ \ell_2\ L\ L_a)$$

In the above N implies addition over the plane wave expansion and contains the expansion coefficients, $p = \sqrt{2p+1}$,

and

$$V^i_{\ell_1 \ell_2 \ell_3} = \int_0^{R_{max}} U_{iA}(r)\ j_{\ell_1}(k_{n_a} r)\ j_{\ell_2}(k_{n_b} r)\ j_{\ell_3}(k_{n_x} r)\ r^2 dr \tag{4.22}$$

and

$$\phi^i_L = \int_0^{R_{max}} \phi(r)\ j_L(s_i r)\ j_L(t_i r)\ r^2 dr \tag{4.23}$$

with

$$s_b = \frac{m_x}{m_a} \cdot k_{n_a} \quad ; \quad t_b = k_{n_x} \tag{4.24}$$

$$s_x = \frac{m_b}{m_a} \cdot k_{n_a} \quad ; \quad t_x = k_{n_b} \tag{4.25}$$

and

$$s_a = \frac{m_x}{m_a} \cdot k_{n_b} \quad ; \quad t_a = \frac{m_b}{m_a} \cdot k_{n_x} \tag{4.26}$$

and we have taken

$$\phi_a(\vec{r}) = \phi(r) \cdot Y_{oo}(\Omega) \tag{4.27}$$

It is quite clear that the integrals (4.22) and (4.23) which appear in place of the radial integrals in the post-form DWBA are very well behaved in contradistinction to the slowly converging integrals of post-form.

4.1 Results of the prior-interaction DWBA approach

In order to test the various aspects of this approach in particular, the finite range aspect and the automatic inclusion of recoil effects, we have studied in detail, the break up of ^{6}Li at 156 MeV on a ^{6}Li target into alpha and deuteron, for which preliminary experimental data[26] on coincidence spectra were available:

$$\underset{a}{^6\text{Li}} + \underset{A}{^6\text{Li}} \rightarrow \underset{b}{\alpha} + \underset{x}{d} + \underset{A}{^6\text{Li}} \tag{4.28}$$

We assumed the target and the projectile to be distinguishable, due to high incident energy and small angles of detection of alpha and deuteron. Thus the angular-correlation for elastic break-up is

$$\frac{d^3\sigma}{d\Omega^L d\Omega_d^L dE^L} = \frac{2\pi \cdot \mu}{\hbar^2 \, k_a} \cdot |T|^2 \quad \rho \tag{4.29}$$

where

$$\rho = \frac{m_A \cdot m_b \cdot m_x \cdot p_b \cdot p_x \cdot h^{-6}}{(m_A+m_x)+m_x(\vec{p}_b-\vec{P})\cdot\vec{p}_x/p_x^2} \tag{4.30}$$

and the symbols have their usual meaning.

The optical potentials used for the analysis are given in Table II, and were obtained by fitting elastic scattering data at appropriate energies.

TABLE II: Optical model potentials

System	V (MeV)	r_o (fm)	a (fm)	W_v (MeV)	r_{ov} (fm)	a_v (fm)
^{6}Li+^{6}Li	59.6	1.66	0.85	1.14	3.12	0.77
α +^{6}Li	88.9	0.99	0.81	4.94	3.00	0.58
d +^{6}Li	78.1	1.05	0.79	8.63	1.28	0.75
α + d*	73.36	1.25	0.65	-	-	-

* Depth adjusted to give a 2 s state bound to 1.47 MeV.

Two alternative descriptions were used for the α-d relative motion wave function in the ground state of the projectile, to get an illustration of the sensitivity of the break up cross section to the details of the internal momentum distribution. In the first instance it was approximated to a Yukawa type function,

$$\phi_{Yuk}(\vec{r}) = N \cdot (e^{-\alpha r}/r) \cdot Y_{oo}(\Omega) \tag{4.31}$$

with

$$\alpha = \sqrt{\frac{2\mu_{\alpha d}\varepsilon}{\hbar^2}} \simeq 0.3066 \tag{4.32}$$

where ε is the binding energy of the projectile and N is the normalization constant. This wave function is implicitly assumed to be valid when the $U(r_{bx}) \cdot \phi(\vec{r}_{bx})$ term in the post-form DWBA T-matrix is replaced by $D_o \delta(\vec{r}_{bx})$ in a zero-range approximation, and implies a Lorentzian form of momentum distribution. The other and more realistic choice was obtain-

ed by generating the (α+d) bound state wave-function in a Woods-Saxon potential well (see table II) giving a 2s state bound to 1.47 MeV. The squares of the Fourier transforms of these two different wave-functions are displayed in fig. 16.

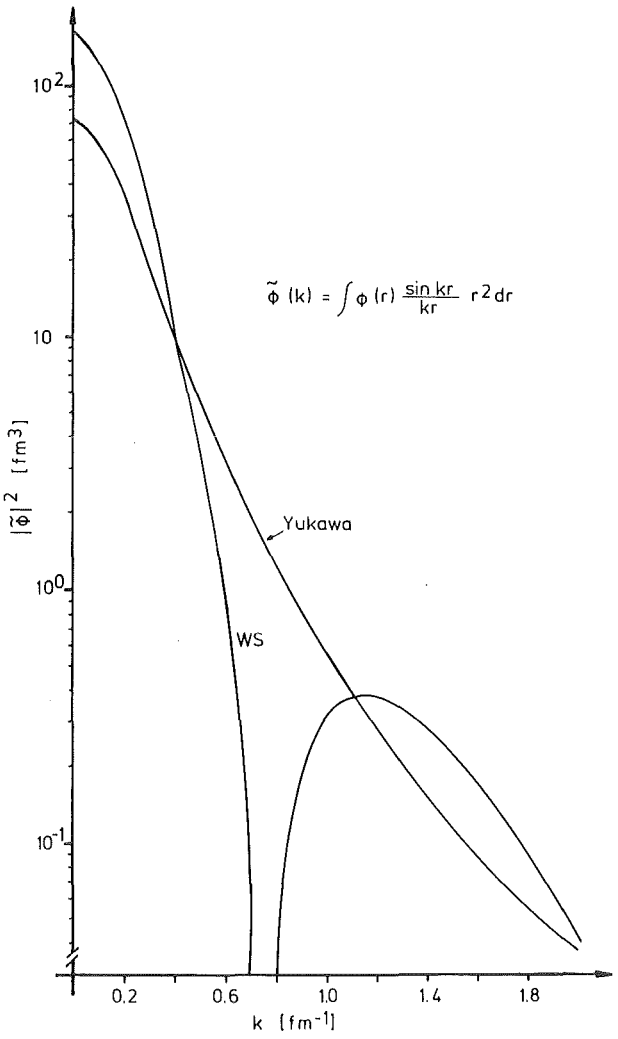

FIGURE 16 Square of the Fourier transform of the α-d relative motion wave-function.

In fig. 17, we present the results for the triple differential cross-section obtained using the Yukawa and the WS wave-functions, for a setting of $\Theta_\alpha^L = 5°$ and $\Theta_d^L = -10°$. As the normalization of the experimental data was uncertain, it has been multiplied by an arbitrary constant to give the peak value as 10 mb/sr² · MeV, for a good perspective. We immediately see that the WS wave-function gives an excellent description of the shape of the angular correlation. Most remarkable is the description of the "shoulder" seen in the data at around 90 MeV of α-particle-energy. These data points correspond to large relative momenta of the fragments and

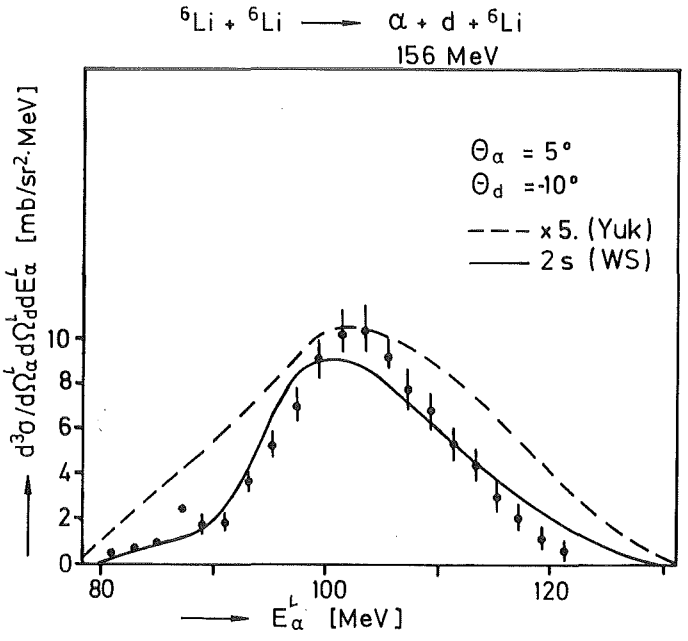

FIGURE 17 The triple differential cross-section for elastic break up of ^6Li in ^6Li+^6Li collisions at 156 MeV.

also involve somewhat larger distortions due to smaller alpha-energies. We see that both these aspects are very well accounted for. On the other hand, the Yukawa function which would be implied by a zero-range approximation (in the post-form) gives only a qualitative description of the data, giving in particular a very large FWHM. This proves that the break up data, especially those corresponding to large relative energies of the fragments are quite sensitive to the details of the relative motion wave function.

In fig. 18 we have plotted the coincidence cross-sections for a situation when the alpha-detector is fixed at 5°, and the cross-section is measured for 105 MeV (∿ beam velocity) alpha particles as a function of the angle of detection of the deuteron.

In addition to plotting the cross-section for the two wave-functions we also give the contribution of the "nuclear break up" and the "nuclear plus Coulomb break up" separately. It is interesting to note that even for such a light target-projectile combination the "Coulomb break up" is substantial.

4.2 The orbital dispersion

If the break up data are to show sensitivity to details of momentum-distribution, most of the contribution to the cross-section should come from the "on-shell-wave-numbers" in the plane-wave expansion of the distorted waves. In order to test this aspect of the "orbital-dispersion" we looked for the percentage contribution of various wave-numbers present in the projectile distorted wave to the cross-section for detection of 105 MeV alpha-particle at $\Theta_\alpha = 5°$ in coincidence with a deuteron emitted at $\Theta_\alpha = -10°$. In the plane wave expansion eighteen terms having wave-numbers between 2.41 fm^{-1} and 5.95 fm^{-1} in steps of 0.27 fm^{-1} were present with vary-

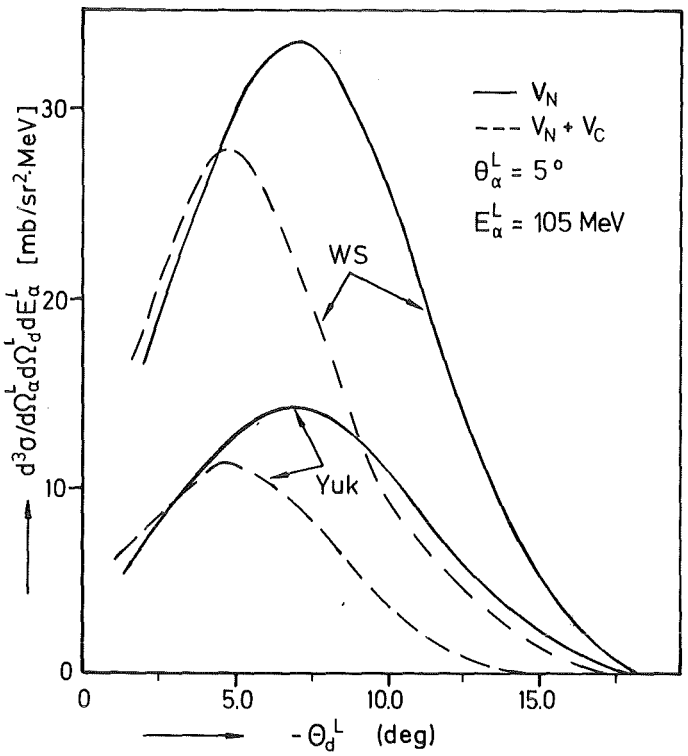

FIGURE 18 The triple differential cross-section for 105 Mev α-particle emitted at $\Theta_\alpha = 5°$ as a function of the emission angle of the deuteron.

ing strengths for different particle waves. However, we found that three wave-numbers closest to the free wave number between them contribute more that 95 % of the cross section, indicating that "orbital dispersion" effects are small.

4.3 The "recombination term" or the simulation of effects of coupling

Before discussing the results of fig. 19, let us have a close look at the expression of the T-matrix in the prior-

form (4.2), by rewriting as,

$$T = \langle \chi_b^{(-)} \chi_x^{(-)} | U_{bA} | \chi_a^{(+)} \phi_a \rangle + \langle \chi_b^{(-)} \chi_x^{(-)} | U_{xA} | \chi_a^{(+)} \phi_a \rangle$$

$$- \langle (\chi_b^{(-)} \cdot \chi_x^{(-)} | \phi_a) | U_{aA} | \chi_a^{(+)} \rangle \qquad (4.33)$$

$$= T_b + T_x - T_a \qquad (4.34)$$

T_b and T_x represent the "shearing" due to the interaction of 'b' and 'x' with the target, respectively. The T_a term can be interpreted to provide the "recombination" as $(\chi_b^{(-)} \cdot \chi_x^{(-)} | \phi_a)$ gives the "projectile-component" of the final state wave-function, $\chi_b^{(-)} \cdot \chi_x^{(-)}$. If the final state were taken as $\chi_a^{(-)} \cdot \phi_{a*}$, where ϕ_{a*} is a continuum state of the projectile, as done by Rybicki and Austern[16], e.g. this term would be identically zero due to the orthogonality of ϕ_a and ϕ_a*.

In fig. 19, we plot the contribution of each of the terms T_b, T_x and T_a along with the full contribution for the same experimental set-up as in fig. 17. We see that the "recombination term" is very large, and plays a very important role in providing the proper description of the experimental data, reproduced very well by the total transition matrix.

We repeated these calculations for the situation $\Theta_\alpha = 5°$ and $\Theta_d = -5°$, and similar results were obtained, though the 'T_x' contribution was higher, understably due to smaller absorption of deuterons, coming out at 5° as compared to 10° in the case above. We also feel that the equivalent post-form DWBA theory of Baur et al.[1] also implicitly includes these coupling effects which should be the reason for its continued success.

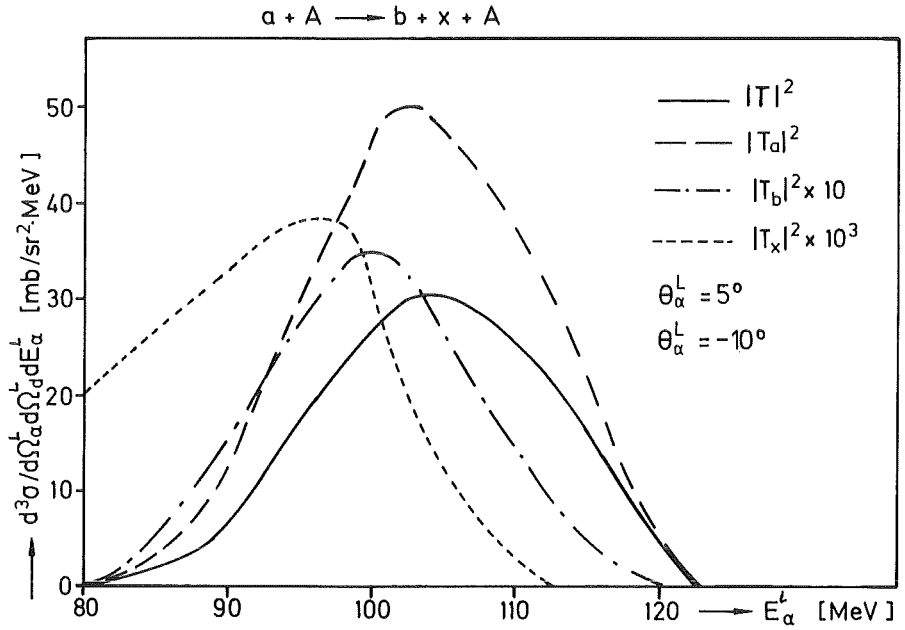

FIGURE 19 Contribution of T_b, T_x and T_a to the cross-section for break up.

4.4 Conclusions on the prior-form approach

In conclusion, we see that the prior-form of the DWBA T-matrix for the direct break up of light ions is amenable to evaluation if the plane-wave expansion technique devised by Robson et al. is used.

When applied to break up of ^{6}Li good results are obtained when a realistic wave-function is used for the relative motion description of alpha and deuteron, showing the unique power of break up data in getting this information. Orbital dispersion effects which are generally believed to camouflage this information are found to be small.

The projectile-target interaction term plays a very important role in describing the data by simulating the "recombination" or the "coupling effects", which are known to be large for break up of light ions.

5. COULOMB BREAK UP

We have already noted the interest in break up of light ions by the Coulomb field of nuclei in providing unique information about reactions of astrophyiscal interest. Coulomb break up is expected to be important if at least one of the following conditions is satisfied:

1) The binding energy of the fragments is small compared to the Coulomb-barrier. This would imply that the energy necessary for break up can be provided, even if the projectile misses the target by a few times the nuclear radius.
2) Special conditions exclude nuclear break up. This would happen for, say, sub-Coulomb energies or for measurements made in the extreme forward angles at higher energies. Such safe angles are possibly limited to angular range within which σ/σ_R is close to unity.
3) Coulomb break up of projectiles would be important even if it is weak for strongly absorbed projectiles, for there is no escape for such particles if the nuclear interaction takes place.
4) The intense virtual photon spectrum for very high energy projectiles may break them up, too. It is expected that a proper DWBA treatment should automatically describe this feature.

Current experiments using the 156 MeV ^{6}Li beam of the Karlsruhe Isochronous Cyclotron, are exploring these conditions. For pure Coulomb break up processes, we have to stick to ex-

treme forward[27] angles, which has become feasible with the commisioning of the magnetic spectrometer "Little John". The relative momentum $\vec{k}$ of b and x, where

$$\vec{k} = \frac{m_x}{m_a} \cdot \vec{k}_b - \frac{m_b}{m_a} \cdot \vec{k}_x \tag{5.1}$$

and $\vec{k}_b$ and $\vec{k}_x$ are their momenta, is kept quite low. This would in turn mean that the energy associated with their relative motion,

$$E_{bx} = \frac{\hbar^2 k^2}{2\mu_{bx}} \tag{5.2}$$

is small compared to the interaction V_{bx} between them, and we should invoke a procedure which treats this final state interaction correctly. This leaves us with the T-matrix advocated by Austern's school.

The other consideration is about the time of contact. One could possibly argue that if the time of contact

$$T > \hbar/\Gamma$$

where Γ is width of the "state" which can be associated with the relative motion of the projectile fragments then one should use Baur's transition matrix, where a transition to the broken up-pair takes place directly from the ground state of the projectile. On the other hand if the time of contact is small compared to such a life time then the sequential picture inherent in Austern's treatment may be more appropriate. The question however, is what width should we associate with nonresonant continuum states. We adopt a view that either due to high energy situation and the fact that we have very distant collisions for pure Coulomb break up, or because possibly the energy of the continuum states provides an order of magnitude value for their width, we are

justified in using this sequential picture. We also assume that the coupling effects which manifest themselves through the requirement of unusual optical model potentials for the exit channel are weak for the Coulomb break up and will not disturb the basic features we wish to explore.

We would also like to state that semi-classical methods will not be quite applicable for such projectiles especially if we wish to explore the differential cross-sections.

5.1 The Coulomb break up T-matrix and its evaluation

With the considerations described above we write the transition matrix for the Coulomb break up as[16]

$$T_{fi}^{Coul} = \langle \chi_{Q_f}^{(-)} \phi_k^{(-)} \mid V_{res} \mid \chi_{Q_i}^{(+)} \phi_a \rangle \tag{5.4}$$

where χ_{Q_i} and χ_{Q_f} are the distorted waves for the projectile and we have

$$\vec{Q}_f = \vec{k}_b + \vec{k}_x \tag{5.5}$$

along with

$$\vec{k} = \frac{m_x}{m_a} \cdot \vec{k}_b - \frac{m_b}{m_a} \cdot \vec{k}_y$$

as give above (5.1). The residual interaction causing the break up is (for $R > r$)

$$V_{res} = 4\pi Z_A \cdot e \sum_{LM \geq 1} \{Z_b (-\frac{m_x}{m_a})^L e + Z_x (\frac{m_b}{m_a})^L e\} \frac{1}{(2L+1)} \cdot Y_{LM}^*(\hat{R}) \cdot Y_{LM}(\hat{r}) \cdot \frac{r^L}{R^{L+1}} \tag{5.6}$$

where

$$\vec{r} = \vec{r}_{bx}$$

and $\vec{R} = \vec{r}_{aA}$ etc. (5.7)

and the symbols have their usual meaning.

Now the T-matrix factorized and yields,

$$T_{fi}^{Coul} = \sum_{LM\geq 1} M^{LM}_{Q_i,Q_f} \cdot M(EL,M,) \tag{5.8}$$

where

$$M^{LM}_{Q_i,Q_f} = Z_A \cdot e \sqrt{\frac{4\pi}{2L+1}} \cdot \langle \chi^{(-)}_{Q_f} | R^{-L-1} Y^*_{LM}(\hat{R}) | \chi^{(+)}_{Q_i} \rangle \tag{5.9}$$

represents an "orbital" matrix and

$$M(EL,M) = \{Z_b(-\frac{m_b}{m_a}\cdot)^L e + Z_x(\frac{m_x}{m_a})^L e\}\sqrt{\frac{4\pi}{2L+1}}$$
$$\langle \phi_k(\vec{r}) | r^L Y_{LM}(\hat{r}) | \phi_a(\vec{r}) \rangle \tag{5.10}$$

represents the "internal" part of the full transition matrix (5.8).

The matrix element (5.9) can be evaluated by making a partial wave expansion of the distorted waves and evaluating the radial integrals numerically. If the wave functions are replaced by pure Coulomb wave functions, the relevant radial integrals are

$$M^L_{L_i,L_f} = \frac{1}{Q_i Q_f} \int_0^\infty F_{L_f}(Q_f \cdot R)\, R^{-L-1}\, F_{L_i}(Q_i \cdot R)\, dR \tag{5.11}$$

which are known analytically from the theory of Coulomb excitation[28]. However, the expression is rather complicated and is obtained by an analytic continuation of Appell's function.

We would like to take this opportunity to suggest an alternative[38], which may be more efficient if the Coulomb-parameter is not too large. We first expand the Coulomb-function in terms of spherical Bessel-functions as fol-

lows[29],

$$F_L(\eta,\rho) = 1.3.5...(2L+1)\rho C_L(\eta) \sum_{k=L}^{\infty} b_k \sqrt{\frac{\pi}{2\rho}}\, J_{k+1}(\rho) \quad (5.12)$$

with

$$b_L = 1, b_{L+1} = \frac{2L+3}{L+1}\,\eta$$

$$b_k = \frac{(2k+1)}{k(k+1)-L(L+1)}$$

$$\{2\, b_{k-1} - \frac{(k-1)(k-2)-L(L+1)}{2k-3}\, b_{k-2}\} \quad (k>L+1) \quad (5.13)$$

and

$$C_L(\eta) = 2^L e^{-\pi\eta/2} \left|\Gamma(L+1+i\eta)\right| \Gamma(2L+2) \quad (5.14)$$

and then use Sonine and Schafheitlin integral[30], to get,

$$\int_0^{\infty} J_\mu(at) J_\nu(bt) t^{-\lambda} dt = \frac{\alpha^\mu \Gamma(\frac{\mu+\nu-\lambda+1}{2})}{2^\lambda b^{\mu-\lambda+1} \Gamma(\frac{-\mu+\nu+\lambda+1}{2}) \Gamma(\mu+1)}$$

$$\times\ {}_\lambda F_1(\frac{\mu+\nu-\lambda+1}{2}\ ,\ \frac{\mu-\nu-\lambda+1}{2};\ \mu+1;\ \frac{a^2}{b^2})$$

$$(\mathrm{Re}(\mu+\nu-\lambda+1)>0;\quad \mathrm{Re}\lambda>-1;\ \alpha \text{ and } b \text{ real};\quad 0<a<b). \quad (5.15)$$

where ${}_\lambda F_1$ is hypergeometric series which reduces to elementary functions in the present case.

6. A PARTICULAR CASE: L = 2 COULOMB BREAK UP

A look at the multipole expansion of the residual interaction for the Coulomb break up (5.6) shows that for projectile having,

$$\frac{Z_x}{m_x} = \frac{Z_b}{m_b} \quad (6.1)$$

$V_{res}(L=1)$ is identically zero. The first major contribution arises from L=2 break up as higher odd modes are suppressed

ed and higher even modes are successively weaker due to the increasing power of R in the denominator. The above situation is realised for

$$^{6}\mathrm{Li} + A \rightarrow \alpha + d + A \tag{6.2}$$

as now the ^{6}Li, α and deuteron move on the same Coulomb-trajectory. In this case, the L = 2 "orbital" matrix (5.9) can be easily evaluated as was pointed out by Serber[31] long ago. We follow these arguments as quoted by Mullin and Guth[32].

First look at the PWBA expression for the orbital matrix,

$$M^{L,M}_{\vec{Q}_i,\vec{Q}_f}(\mathrm{PWBA}) = Z_A \cdot \sqrt{\frac{4\pi}{2L+1}} \cdot \int \frac{e^{i\vec{q}\cdot\vec{R}}}{R^{L+1}} \cdot Y_{LM}(\hat{R})\, d\vec{R} \tag{6.3}$$

where

$$\vec{q} = \vec{Q}_i - \vec{Q}_f \tag{6.4}$$

In writing (6.3), it is assumed that the multipole expansion (5.6) is valid for all values of R. We shall come to this later again.

Now, taking the z-axis along $\vec{q}$ we get

$$\begin{aligned} M^{L,M}_{\vec{Q}_i,\vec{Q}_f}(\mathrm{PWBA}) &= 4\pi \cdot Z_A \cdot e \cdot q^{L-2} \lim_{R_o \to 0} \left[\frac{j_{L-1}(qR_o)}{(qR_o)^{L-1}} \right] \\ &= 4\pi \cdot Z_A \cdot e \cdot \frac{q^{L-2}}{(2L-1)!!} \end{aligned} \tag{6.5}$$

This matrix element has the endearing property of being independent of $\vec{q}$, $\vec{Q}_i$ and $\vec{Q}_f$ for L = 2. Introducing the Fourier transforms of the scattering states

$$\chi_{\vec{Q}_i}(\vec{R}) = \int \tilde{\chi}_i(\vec{k})\, e^{i\,\vec{k}_i\cdot\vec{R}}\, d\,\vec{k}_i \tag{6.6}$$

and

$$\chi^{(+)}_{\vec{Q}_f}(\vec{R}) = \int \tilde{\chi}_f(\vec{k}_f)\, e^{i\,\vec{k}_f\cdot\vec{R}}\, d\,\vec{k}_f \qquad (6.7)$$

we get for the orbital matrix (5.9)

$$M^{LM}_{\vec{Q}_i,\vec{Q}_f} = \int d\vec{k}_i\, d\vec{k}_f \cdot M^{LM}_{\vec{k}_i,\vec{k}_f}(\text{PWBA}) \cdot \tilde{\chi}_i(\vec{k}_i) \cdot \tilde{\chi}^*_f(\vec{k}_f) \qquad (6.8)$$

which for L = 2 yields,

$$M^{L=2}_{\vec{Q}_i,\vec{Q}_f} = M^{L=2}_{\vec{Q}_i,\vec{Q}_f}(\text{PWBA}) \int d\vec{k}_i \tilde{\chi}_i(\vec{k}_i) \cdot \int dk_f \cdot \tilde{\chi}^*_f(\vec{k}_f)$$

$$= M^{L=2}_{\vec{Q}_i,\vec{Q}_f}(\text{PWBA}) \cdot \chi_i(\vec{R}=o) \cdot \chi^*_f(\vec{R}=o) \qquad (6.9)$$

We see that the orbital matrix element for the L = 2 Coulomb break up reduces to a "contact term" provided by the value of the wave function at the origin. Making a partial wave expansion of the distorted waves involved, we get,

$$M^{L=2}_{\vec{Q}_i,\vec{Q}_f} = M^{L=2}_{\vec{Q}_i\cdot\vec{Q}_f}(\text{PWBA}) \cdot \left[\frac{u^i_o(Q_i R)}{Q_i R}\right]_{R=o} \cdot \left[\frac{u^f_o(Q_f R)}{Q_f R}\right]_{R=o} \qquad (6.10)$$

where u^i_o and u^f_o are the radial wave functions of s-partial waves. Obviously, the use of correct distorted waves modifies the PWBA cross section just by a factor, C^2, where

$$C^2 = \left|\chi^{(+)}_{\vec{Q}_i}(\vec{R}=o) \cdot \chi^{(-)*}_{\vec{Q}_f}(\vec{R}=o)\right|^2 \qquad (6.11)$$

As the above expression is so simple, we would like to recall the assumptions which made it possible. The most important is the assumption that the multipole expansion of the residual interaction is given as r^L/R^{L+1} over the entire

range of R, which is strictly valid only for R>r. We first note that due to the bounded nature of the projectile wave function ϕ_a, only small values of r are relevant, where as the long-range nature of the Coulomb-force entails contributions from large values of R. One other aspect becomes more clear, if we visualize a partial wave expansion of the distorted waves and subsequent integration. We note that low partial waves which are very strongly absorbed will not contribute to the matrix element. The partial waves having larger L-values deviate significantly from zero only for large values for R. These two features would insure that significant contributions accrue to the transition matrix only from large values of R insuring the validity of our approximation. However, these considerations also imply that the contact term C^2 has to be calculated with proper distorted waves derived from a Coulomb potential of a realistic charge distribution and adequate nuclear potentials accounting for absorption effects. The corresponding wave functions can be easily provided from any optical model scattering code. The essentiality of using proper scattering wave-functions can be easily demonstrated by noting that for a point-charge nucleus without nuclear potential,

$$C^2 = \left|\overline{2\pi\eta_i/(e^{2\pi\eta_i}-1)}\right| \cdot \left|\overline{2\pi\cdot\eta_f/(e^{2\pi\eta_f}-1)}\right| \qquad (6.12)$$

with the Coulomb parameter,

$$\eta_{i,f} = Z_p \cdot Z_A \cdot e^2/\hbar\, v_{i,f} \qquad (6.13)$$

and for say 156 MeV ^{6}Li incident on ^{208}Pb, it is as low as 0.36×10^{-38} implying an extremely low Coulomb break up cross-section for this situation.

6.1 Theoretical predictions of the triple differential cross-section

As stated earlier, we shall discuss in detail the specific case of *elastic* break up of 156 MeV ^{6}Li in the Coulomb field of ^{208}Pb. We consider various laboratory conditions for the emission of α-particles and deuterons (Θ_α^L, Θ_d^L, E_α^L). The relative angle $\Delta\Theta$ defines the minimum value of the relative momentum k obtainable in a particular kinematic consideration. Fig. 20 displays the variation of the relative momentum k with the energy of the α-particle fragment, which is coincidently observed with the fragment deuteron, while the target nucleus remains in the ground state (elastic break up).

The evaluation of the full matrix element (5.8) for L=2 requires a specification of the wave functions $\phi_{Li}(r)$ and ϕ_k. The ground state wave function is generated by a bound-state potential of Saxon-Woods form reproducing the binding energy while the nonresonant continuum states were generated in the α-d potential given by McIntyre and Haeberli[33] (see also Robertson et al.[34]).

The internal part of the matrix elements can be written as,

$$M(E2,M) = \sqrt{\frac{4\pi}{5}} \{Z_\alpha e (\frac{m_d}{m_{Li}})^2 + Z_d e (\frac{m_\alpha}{m_{Li}})^2 \} * \langle \phi_k | r^2 Y_{LM} | \phi_{Li} \rangle \qquad (6.14)$$

which is related to the reduced transition probability (De Shalit and Talmi[35])

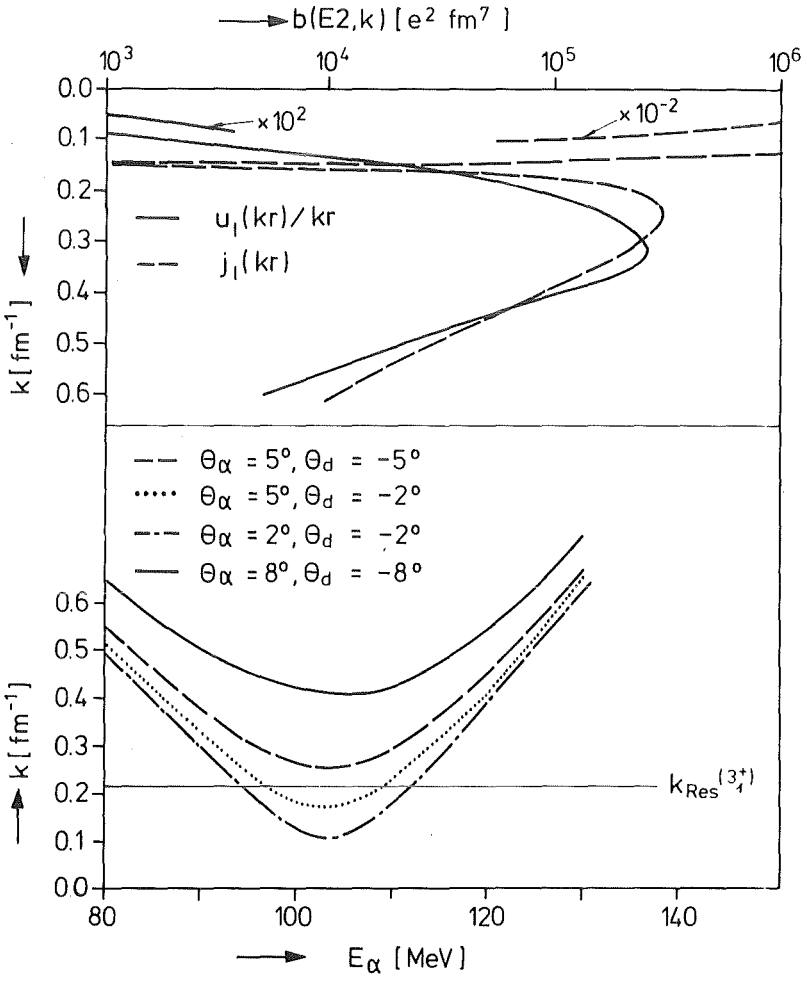

FIGURE 20 Variation of the relative α-d momentum k with the observed α-particle energy E^{Lab} in the elastic break up of 156 MeV-^{6}Li ions, and the nonresonant b(E2,k) distribution

$$b(EL,k,J_i \to J_f) = \{Z_\alpha e(\frac{m_d}{m_{Li}})^2 + Z_d e(\frac{m_\alpha}{m_{Li}})^2\}^2 \; * \;$$

$$\frac{(2J_f+1)(2\ell_i+1)(2\ell_f+1)(2L+1)}{4\pi} \; *$$

$$\begin{Bmatrix} \ell_i & \ell_f & L \\ 0 & 0 & 0 \end{Bmatrix}^2 \begin{Bmatrix} \ell_f & \ell_i & L \\ J_i & J_f & S_f \end{Bmatrix}^2 |<R^L>|^2 \qquad (6.15)$$

We denote

$$<R^L> = 4\pi \; i^L \sqrt{\frac{2L+1}{4\pi}} \int_0 -\frac{u_{\ell_f}(kr)}{kr} r^2 \; \Phi_{Li}(r) r^2 \, dr \qquad (6.16)$$

with Φ_{Li} being the radial part of ϕ_{Li}, $u_{\ell_f}(kr)/kr$ the same for the continuum states. For the case of the $1^+_{gr} \to 3^+_1$ transition in ^{6}Li (ℓ_i=0, ℓ_f=2, S_f=1, L=2) we get

$$b(E2,k,1^+ \to 3^+) = \{Z_\alpha e (\frac{m_d}{m_{Li}})^2 + Z_d e(\frac{m_\alpha}{m_{Li}})^2\}^2$$
$$* \frac{7}{12\pi} |<R^2>|^2 \qquad (6.17)$$

The quantity b(E2,k) represents a transition density (in units of e^2 fm^7) and is displayed in fig. 20. For comparison, the b(E2,k) distribution is additionally calculated by using plane waves for describing the continuum states. It is obvious that at low k-values considerable differences occur as compared to the use of more correct scattering states, primarily due to the Coulomb repulsion. The triple differential cross section

$$\frac{d^3\sigma}{d\Omega_\alpha d\Omega_d dE_\alpha} = \frac{2\pi\mu}{\hbar^2 Q_i} \frac{1}{2J_i+1} \sum_{M_i M} |T_{fi}|^2 \cdot \rho \qquad (6.18)$$

with ρ being the three body phase space factor (4.30) can be concisely written as

$$\frac{d^3\sigma}{d\Omega dE_\alpha} = \frac{(4\pi)^4}{90\,\hbar} \frac{Z_A^2\, e^2}{(2J_f+1)} \sqrt{\frac{m_{Li}}{E_{1i}^{Lab}}}\, C^2\, b(E2,E)\rho \qquad (6.19)$$

(E relative energy of the fragments)

as

$$\frac{1}{2J_i+1} \cdot \sum_{M_i M} |\Gamma_{if}|^2 = \left|\frac{\overline{4\pi}}{3} Z_A e\right|^2 \cdot \frac{1}{2J_f+1} \left(\frac{4\pi}{5}\right) b(E2,E) \qquad (6.20)$$

Figs. 21-23 show the nonresonant triple differential cross-section for some pairs of emission angles. The results in fig. 21 differ by the values of the penetration factor C^2 which are calculated with a spherical homogeneous charge distribution ($R_c = 1.3\, A_{Target}^{1/3}$) only and with optical model parameters of a Saxon-Woods form as given in Ref. 13.

Fig. 24 displays the variation of various factors with the laboratory energy of the α-particle observed in a particular kinematical arrangement of the detectors.

In fig. 25 the resonance excitation of the 3_1^+ state in ^{6}Li ($k_{res} = 0.21\ fm^{-1}$) is included with a width Γ (= 26 keV) corresponding to B(E2; $1^+ - 3_1^+$) = 45 e^2 fm^4 (Endt[39] by writing

$$B(EL,J_i \to J_f) = \frac{1}{(2\pi)^3} \int b(EL,k,J_i \to J_f)\, |f|^2 \cdot k^2\, dk \qquad (6.21)$$

Here

$$|f|^2 = \left|\frac{i\,\Gamma/2}{(E-E_{res})+i\Gamma/2}\right|^2 \qquad (6.22)$$

is a Breit-Wigner resonance factor with $E = \hbar^2 k^2 / 2\mu_{\alpha d}^{\alpha}$ and $E_{res} = \hbar^2\, k_{res}^2 / 2\mu_{\alpha d}$. For the very narrow 3_1^+ resonance we replaced

$$B(EL,J_i \to J_f)_{Res} = \frac{\mu_{\alpha d}\, k_{res}}{(2\pi)^3 \hbar^2}\, b(EL,\, k_{res}) \cdot \pi \cdot \frac{\Gamma}{2} \qquad (6.24)$$

The result shown in Fig. 25 demonstrates the dominance of the "sequential break up" via the 3_1^+ resonance. However,

the resonance peak disappears in other kinematical arrangements (see fig. 20).

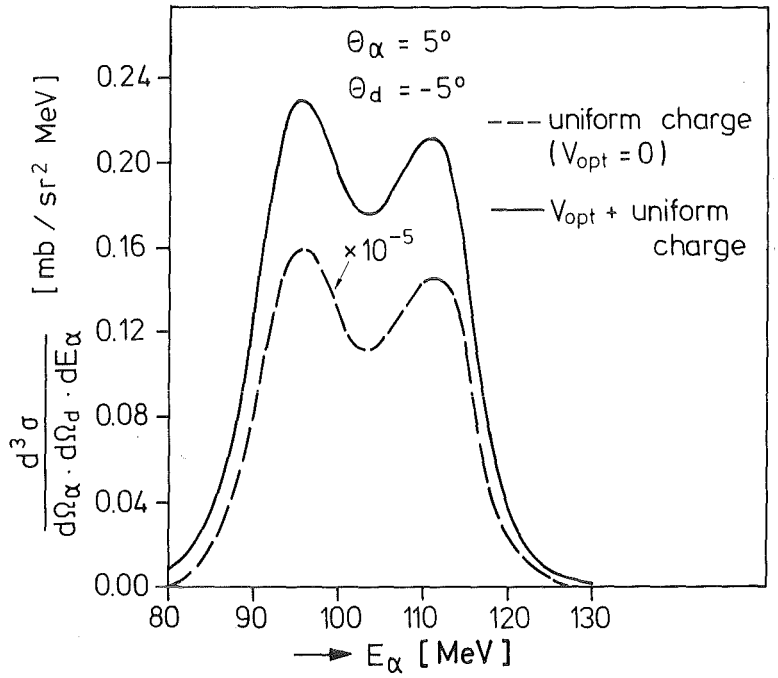

FIGURE 21 Triple differential cross section and shape of the correlated α-particle spectrum in the non-resonant $^{208}Pb(^6Li,\alpha d)^{208}Pb$ break up reaction at E_{Li} = 156 MeV.

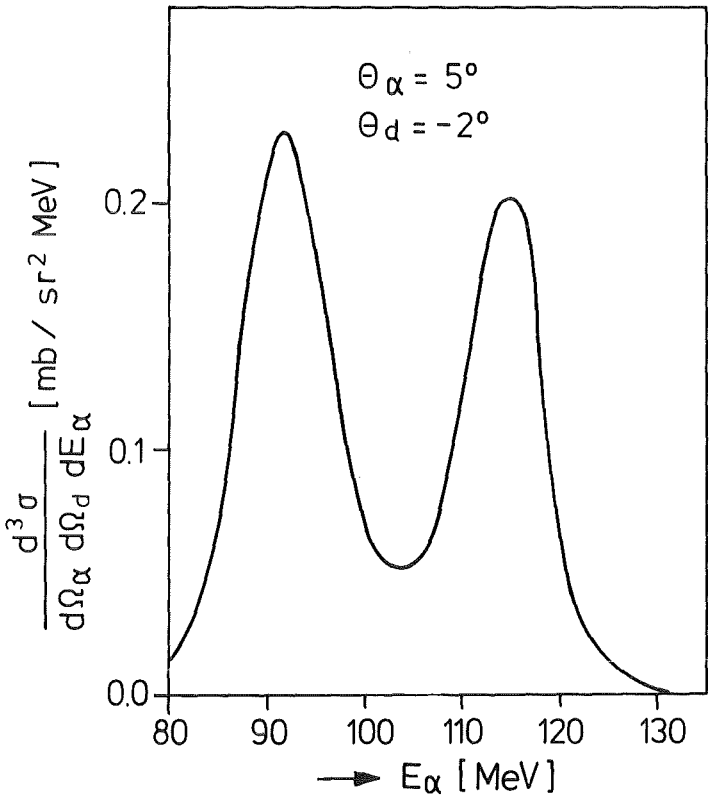

FIGURE 22 Triple differential cross section of the nonresonant $^{208}Pb(^{6}Li,\alpha d)^{208}Pb$ reaction

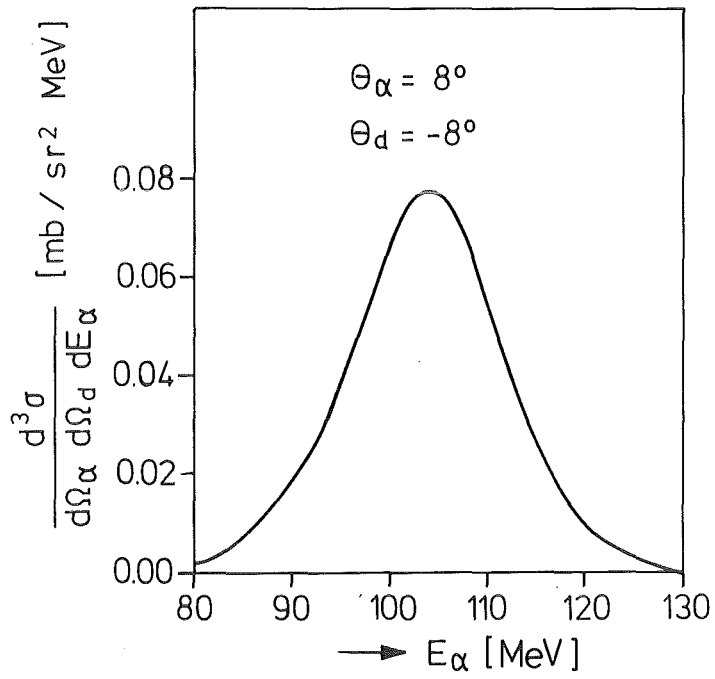

FIGURE 23 Triple differential cross section of the non-resonant $^{208}Pb(^{6}Li,\alpha d)^{208}Pb$ reaction

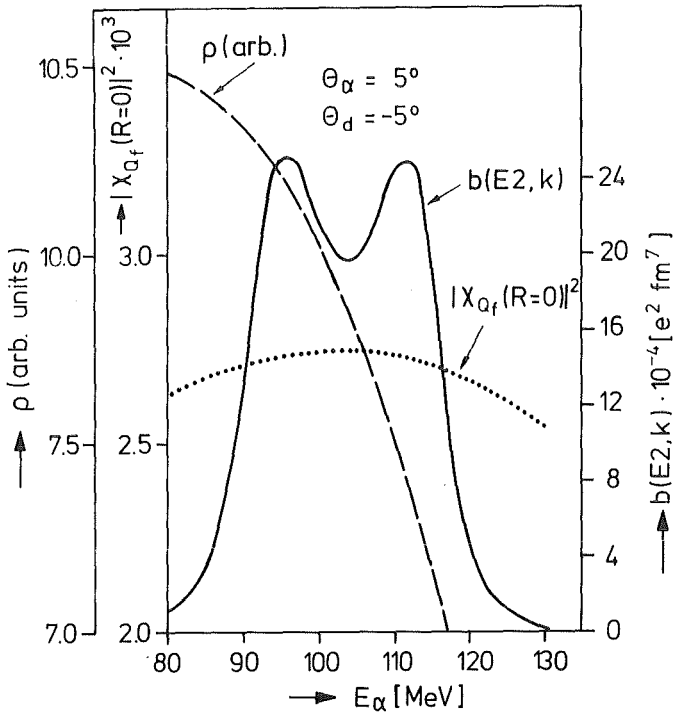

FIGURE 24 The variation of the phase space factor ρ, of the contact term ($\propto|\chi_{Qf}(R=0)|^2$) and of the reduced transition probability with the α-particle energy

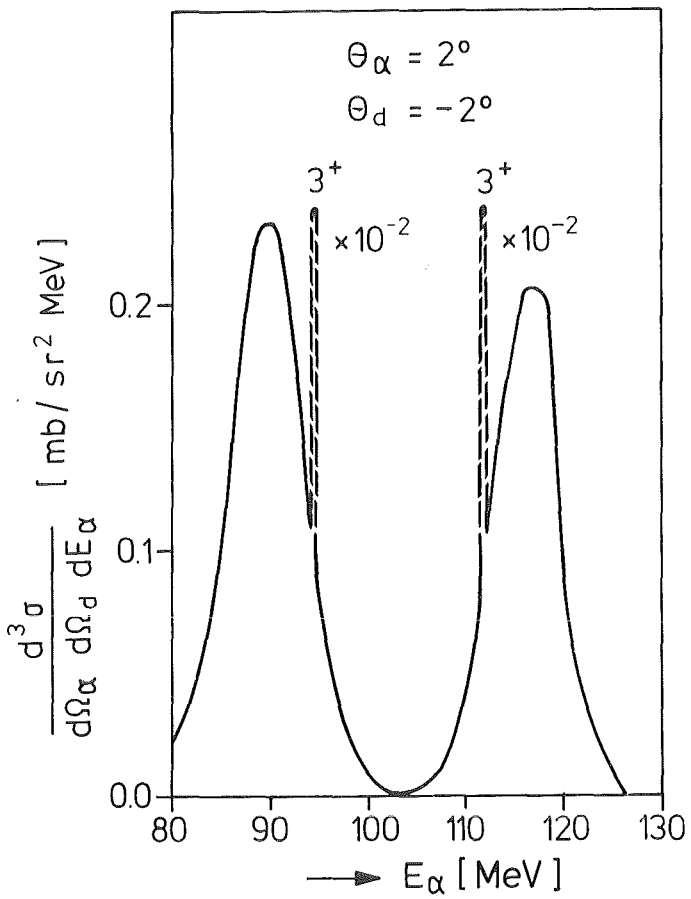

FIGURE 25 Resonant and nonresonant excitation of the α-d continuum in ^{6}Li by projectile break up in the Coulomb field of ^{208}Pb at E_{Li} = 156 MeV

7. CONCLUSIONS AND OUTLOOK

We have seen that the break up of composite particles in the nuclear and Coulomb field of nuclei is a promising field, playing a crucial role in providing accurate information about nuclear reaction of astrophysical interest, in addition to relevant information about the internal momentum distribution and the cluster structure of the projectile. Two explicit situations emerged: One in which the final state interaction of the resulting fragments could be ignored, and the other when the relative energy between the fragments is small, implying a strong final state interaction.

The appropriate DWBA T-matrix for the first case is provided by the Baur's school as

$$T_{fi} = \langle \chi_b^{(-)} \cdot \chi_x^{(-)} \; | V_{bx} | \; \chi_a^{(+)} \cdot \phi_a \rangle \qquad (7.1)$$

which can be evaluated using contour integration, if a zero-range approximation is introduced. This approximation further compromises the final state interaction and in addition imposes the restriction that the internal motion of the projectile is limited to s-state with a momentum distribution of a Lorentzian shape.

If the equivalent prior-form is used then

$$T_{fi} = \langle \chi_b^{(-)} \cdot \chi_x^{(-)} \; | U_{bA}+U_{xA}-U_{aA} | \; \chi_a^{(+)} \; \phi_a \rangle \qquad (7.2)$$

and the restriction about the projectile wave-function is easily dispensed with. The problem of accurate treatment of the final state interaction still remains.

The T-matrix of the Austern's school

$$T_{fi} = \langle \chi_a^{(-)} \cdot \phi_k^{(-)} \; | U_{bA}+U_{xA}-U_{aA} | \; \chi_a^{(+)} \; \phi_a \rangle \qquad (7.3)$$

on the other hand has no such limitations on the projectile

wave-function and treats the final state interaction to all others. It, however, has the uncertainty associated with the proper choice of the optical potential (U_{aA}) for the exit channel distorted waves $\chi_a^{(-)}$.

Nevertheless, the use of (7.3) for Coulomb break up of ^{6}Li yields expressions of remarkable simplicity and provides valuable estimates for cross-sections for very low α-particle-deuteron ralative energies. The nonresonant break up cross-section is found to be large, though if permissible within the three-body kinematics the break up through the 3_1^+ resonance state dominates.

We have not discussed theories of inclusive measurements which are a subject of a debate now. They provide less clear physical information as the observables are averaged over a large number of channels.

The future should witness detailed measurements of the break up phenomena, both inclusive and exclusive, the later measurements being performed both in and out of reaction plane. There are indications that experiments performed with polarized beams may provide more direct information about the reaction mechanism, through the measurements of the analysing power. Experiments performed with projectiles whose ground states are different from s-states may provide useful information about the intrinsic angular momentum dependence of the break up mechanism. Experiments performed with one of the detectors put at a forward angle and the other one at varying angles are expected to reveal the evolution of the break up process possibly as a pure Coulomb in the extreme forward angles, nuclear plus Coulomb at grazing angles, nuclear at higher angles and more complicated processes at still higher angles. The verification of some of these concepts is expected to use up a considerable part of the future endeav-

ours in the studies of break up phenomena.

Then, we have the important problem of experimental verification of ideas leading to reliable values of cross-sections for astrophysics.

The developments in theory are expected to provide answers for the requirement of unusual optical model potentials in the exit channel or an alternative post-form of DWBA theory which includes final state interactions to all orders. The amazing question also remains about the relationship of the two schools of break up.

Here a comment must be made of the work of Kamimura and coworkers[36] which provides some answer to many of the questions raised above and is a step in the right direction. However, for the moment it does not include break up due to the Coulomb field and the coupled discretized continuum channels calculations can be hardly performed in a simple routine manner as it has become possible for the DWBA methods discussed.

Break up studies with a heavy target also provide us with a means to test the extent to which the unsolvable three body situation can be approximated by soluable two body situation within the framework of the DWBA.

In view of these perspectives the projectile break up in the Coulomb and nuclear field it is a rich field with possibilities for innovative experimentation and bold theoretical concepts. We should not forget that we are dealing with a three body situation, one of the first one to be studied in such great detail, and we should be prepared for pleasant surprises.

ACKNOWLEDGEMENTS

It is a pleasure for me to thank for the kind hospitality of Prof. Dr. G. Schatz and Prof. Dr. H. Rebel at Kernforschungszentrum Karlsruhe where the work presented in these lectures was done. My special gratitude is to Prof. Rebel who collaborated with me on all these investigations and who carefully read the manuscript and prepared it for publication. Finally, I would like to thank Prof. Z. Wilhelmi and the Organizing Committee of the 17th International Summer School on Nuclear Physics for their kind invitation and hospitality at Mikołajki.

REFERENCES

1. G. BAUR, F. RÖSEL, D. TRAUTMANN and R. SHYAM, Phys. Rep. C111, 333 (1984).
2. R.I. DE MEIJER and R.KAMERMANS, Rev. Mod. Phys. 57, 147 (1985).
3. R. SERBER, Phys. Rev. 72, 1008 (1947).
4. See e.g. M.N. HARAKEH, 17th International Summer School On Nuclear Physics, Mikolajki, Poland, Sept. 1985.
5. H. REBEL, "Nuclear Reaction Cross Sections of Astrophysical Interest", Unpublished Report, Kernforschungszentrum Karlsruhe (1985).
6. G. BAUR, Private Discussion
7. L. JARECZYK, I. LANG, R. MÜLLER, D. BALZER, P. VIATTE and P. MARMIER, Phys. Rev. C8, 68 (1973).
8. N. MATSUOKA, M. KONDO, K. HATANAKA, T. SAITO, T. ITAHASHI, K. HOSONO, A. SHIMIZU, F. OHTANI, and O. CYNSHI, Nucl. Phys. A391, 357 (1982).
9. E.H.L. AARTS, R.A.R.L. MALFLIET, R.I. DE MEIJER and S.Y. VAN DER WARF, Nucl. Phys. A425, 23 (1984)
10. N. MATSUOKA, A. SHIMIZU, K. HOSONO, T. SAITO, M. KONDO, H. SAKAGUCHI, A. GOTO and F. OHTANI, Nucl. Phys. A397, 269 (1980).
11. A. BUDZANOWSKI, G. BAUR, R. SHYAM, I. BOJOWALD, W. OELERT, G. RIEPE, M. ROGGE, P. TUREK, F. RÖSEL and D. TRAUTMANN, Z. Physik A393, 293 (1979).
12. J. UNTERNÄHRER, I. LANG, and R. MÜLLER, Phys. Rev. Lett. 40, 1077 (1978).
13. B. NEUMANN, H. REBEL, H.J. GILS, R. PLANETA, J. BUSCHMANN, H. KLEWE-NEBENIUS, S. ZAGROMSKI, R. SHYAM and H. MACHNER, Nucl. Phys. A382, 296 (1982).
14. B. NEUMANN, H. REBEL, J. BUSCHMANN, H.J. GILS, H. KLEWE-NEBENIUS and S. ZAGROMSKI, Z. Phys. A296, 113 (1980).
15. A. POP et al., Contrib. XVIIth Int. Summerschool on Nuclear Physics, Mikolajki, Poland, Sept. 1985 - Private communications O. KARBAN, ibid.
16. F. RYBICKI, and N. AUSTERN, Phys. Rev. C6, 1525 (1971).
17. T. UDAGAWA, and T. TAMURA, Phys. Rev. C21, 1271 (1980).
18. A. GOTO, H. KAMITSUBO, H. SAKAGUCKI, F. OHTANI, N. MATSUOKO, A. SHIMIZU, K. HOSONA, T. SAITO, M. KONDO, and S.I. HAYAKAWA, International Symposium on Highly excited states in Nuclear Reactions, edited by H. AKEGAMI and N. MATSUOKA, Research Centre for Nuclear Physics, Osaka, Japan (1980) p. 65.
19. R. HUBY and J.R. MINES, Rev. Mod. Phys. 37, 406 (1965).
20. H. AMAKAWA and N. AUSTERN, Aust. J. Phys. 36, 633 (1983) and Refs. therein.

21. N. AUSTERN, Phys. Rev. C30, 1130 (1984).
22. P. BRAUN-MUNZINGER, H.H. HARNEY and S. WENNES, Nucl. Phys. A235, 190 (1974).
23. G. BAUR and D. TRAUTMANN, Phys. Rep. C25, 293 (1976)
24. D.K. SRIVASTAVA and H. REBEL, Invited talk given at 4th International Conference on Nuclear Reaction Mechanisms, 10-15 June, 1985, Varenna (Como) - Italy
25. D. ROBSON and R.D. KOSHEL, Phys. Rev. C6, 1125 (1972), L.A. CHARLTON, Phys. Rev. C8, 146 (1973).
26. S. MICEK, private communication.
27. H.J. GILS, KfK-Report 2972 (1980).
28. K. ALDER, A. BOHR, T. HUNS, B. MOTTELSON and A. WINTHER, Rev. Mod. Phys. 28, 432 (1956).
29. M. ABRAMOWITZ and I.A. STEGUN, Handbook of Mathematical Functions, Dover Publications, New York, 540 (1964).
30. Ibid, p. 487.
31. Quoted as ref. 12 in ref. 32.
32. C.J. MULLIN and E. GUTH, Phys. Rev. 82, 141 (1951)
33. L.C. McINTYRE and W. HAEBERLI, Nucl. Phys. A91, 382 (1967).
34. R.G.H. ROBERTSON, P. DYER, R.A. WARNER, R.C. MELIN, T.J. BOWLER, A.B. McDONALD, G.C. BALL, W.G. DAVIES and E.D. EARLE, Phys. Rev. Lett. 47 (1981) 1867
35. A. DE SHALIT and I. TALMI, Nuclear Shell Theory, Academic Press (1963).
36. Y. SAKURAGI, M. YAHIRO and M. KAMIMURA, Prog. Theoret. Phys. 70, 1047 (1983).
37. D.K. SRIVASTAVA and H. REBEL, 4th. Int. Conf. on Nuclear Reaction Mechanisms, 10-15 June, 1985, Varenna (Como) - Italy.
38. C. SAMANTA, D.K. SRIVASTAVA and H. REBEL, Unpublished Results, Kernforschungszentrum Karlsruhe 1985.
39. P.M. ENDT, Atomic Data and Nucl. Data Tab. 23, 3 (1979).